

Department of Construction Sciences
Solid Mechanics

ISRN LUTFD2/TFHF-24/5259-SE(1-58)

Verification of FEM-models of dynamic strain in bolts during recoil

Master's Dissertation by
Martina Grövnäs

Supervisors:
Jonas Engqvist, Division of Solid Mechanics
Linus Ludvigsson, Aimpoint AB
Jacopo Gili, Aimpoint AB

Examiner:
Mathias Wallin, Division of Solid Mechanics

Copyright © 2024 by the Division of Solid Mechanics
and Martina Grövnäs

Printed by Media-Tryck AB, Lund, Sweden

For information, address:

Division of Solid Mechanics, Lund University, Box 118, SE-221 00 Lund, Sweden

Webpage: www.solid.lth.se

Abstract

When creating finite element simulations, fasteners are often simplified or disregarded even though they are exposed to large loads and are reasons to cause failure in the model. Aimpoint AB produces electronic red dot sights that are exposed to high accelerations of at least 400G. The aim of this degree project is divided into two parts: develop and evaluate a test methodology for measuring strain in bolt during high recoils with the help of embedded strain gauges, and to confirm if finite element simulations of the bolts is a reliable method to verify that they are suited for recoil exposure. The simulations will focus on three different methods of modeling a bolt: a coupled-, a hybrid- and a solid bolt. These will contribute to further development of design choices and dimensioning of fasteners, test development of strain measurements and overall time efficiency for Aimpoint.

The project consists of two studies to reach the goals. The first study is to create a test method to verify the use and behavior of strain gauges, which then leads to the second study of using the strain gauges in recoil tests. The test methodologies for both studies were successful and will contribute to further understanding of testing bolts in high recoil environments with the help of strain gauges. On the other hand, the simulations of the shock tests were not reliable despite which bolt model was used and will require further investigation. The models resulted in strain curves that were two to three times larger than during the experiments. Using the simulations to develop test will give a substantial margin of error that the designs will not be sufficiently tested. With greater knowledge of the simulation program and continued work on the bolt models, there is hope to develop a more reliable simulation.

Acknowledgment

I would like to express my deepest gratitude for getting the opportunity to complete my M.Sc. in Engineering Physics at the division of Solid Mechanics at LTH and at Aimpoint AB in Malmö. I am very grateful for Aimpoint AB for providing the necessary equipment, support and great colleagues. A special thank you to my supervisors, Jacopo Gili and Linus Ludvigsson at Aimpoint and Jonas Engqvist at LTH, for your guidance and support. Grazie mille Jacopo for pushing me to be more curious and to not give up too easily. An extended gratitude goes out to Loke Sundblad and Viktor Wiese for the support in the lab and the FEM-simulations respectively.

Lund, May 2024
Martina Grövnäs

Contents

1	Introduction	1
1.1	Aimpoint	1
1.2	Background	1
1.3	Aim and Objective	1
1.4	Limitations	2
1.5	Report structure	2
2	Theory	3
2.1	Load cases and their FEM solver counterpart	3
2.2	FEA of bolt models	3
2.3	Mass scaling	6
2.4	Material characteristics	6
2.5	Strain gauge	7
2.6	Wheatstone bridge	9
2.7	Piezoresistive accelerometer	10
3	Abaqus glossary	11
4	Method	15
4.1	3D modeling	15
4.2	Initial FEM simulations	16
4.2.1	Quasi-static simulation	16
4.2.2	Dynamic simulation	17
4.3	Preparations	18
4.4	Tests	22
4.5	FEM verification of recoil test	25
5	Results - Quasi-static study	28
5.1	3D modeling	28
5.2	Initial FEM simulation	29
5.3	Tests	30
6	Results - Dynamic study	32
6.1	3D modeling	32
6.2	Initial FEM simulation	33
6.3	Tests	35
6.4	FEM verification of recoil test	39
7	Discussion	44
7.1	Test methodology	44
7.2	FEM-verifications of bolts during recoil	44
7.3	Sources of error	45
7.4	Future work	46

8	Conclusion	47
9	Appendix	50

1 Introduction

1.1 Aimpoint

Aimpoint AB, founded in 1975, is the originator and the now global leader of the electric red dot sight. The sight was originally made for hunters and sport shooters but has since then expanded to police and military use [1]. Aimpoint conducts many vigorous tests to be able to deliver high quality sights which can withstand high forces of recoil, shock, pressure and vibration as well as environmental forces such as water depths, deterioration and extreme temperatures. Prior to conducting dynamic tests, an FEA (Finite Element Analysis) can be used to verify if the sight will stay intact or break. However, how certain are they that the simulations are comparable to reality?

The project idea originated from Aimpoint AB and the following results were derived at their headquarters in Malmö. Regardless of the result, this project will assist with overall time efficiency for the company by alleviating others from duplicating errors when continuing the work or by implementing the successful project. In addition to this, a successful result will aid in method development for dynamic modeling and testing.

1.2 Background

Design optimization by Finite Element Method (FEM) modeling often consists in a series of simplifications and assumptions which needs to be made to optimize the process. Fasteners are elements of a design which tends to be simplified by idealized elements in FEM modeling. However, they are, at the same time, exposed to quite large, dynamic loads and possibility of failure can often cause large effect on the product. When the actual conditions during recoil are known it is possible to better optimize the design based on FEM models which can give reduction both in weight and material as the fasteners can be dimensioned in an effective way. A deep knowledge of the actual conditions which develops in the scenario which needs to be modeled is key for comparison to model data; which if correctly estimated, can lead to a safe assessment of possible risks associated the modeled design and assessment of their mitigation.

1.3 Aim and Objective

The aim of this master's project was to:

1. Evaluate the testing method of embedded strain gauges in bolts and develop a reliable measurement technique of strain during recoils of different magnitudes.
2. Answer if FEM-modeling of fasteners can be a reliable method to verify that designs are suited for recoil exposure.

A successful thesis will advance the development of dimensioning of fasteners in areas exposed to high intermediate stress. A successful method development will allow

for better understanding of design choices when fasteners are exposed to recoils and could give insight in how to further develop strain measurements during recoils.

1.4 Limitations

To fulfill the aim of the thesis there are countless ways to model a bolt in a FEM simulation, but to limit the scope of this project, three main models were chosen. These vary in how much of a solid bolt is included. The three models are called solid bolt, hybrid bolt and coupled bolt.

1.5 Report structure

The project is separated in two studies: one quasi-static and one dynamic. The quasi-static test consists of a tensile test while the dynamic test is a recoil test. As will be mentioned later on, both studies have a similar methodology but differ in end goals. The methodology will therefore be described together and then be separated in the results as they were conducted one study at a time. The results of the first study determines the start of the next. Further, the quasi-static study is divided into two parts. The first part is to test a general linear strain gauge in the tensile machine and the second part is to conduct the same test but with a strain gauge embedded into a bolt. The same type of bolt is then to be used in the dynamic test. For easier reading there will be a glossary attached, which can be found on page 11.

2 Theory

This section will delve deeper into the main topics of this project to give an understanding when they are presented further into the report. The topics include methods used in finite element analysis, material properties and measuring equipment.

2.1 Load cases and their FEM solver counterpart

The definition of quasi-static loading is that the load is applied to a structure in a steady and slow manner, almost statically i.e. no time dependency, and therefore any inertia force caused by the load can be neglected [2]. For these cases, it is reasonable to make use of an implicit solver. An implicit solver, also known as Abaqus/Standard in the program used, solves for static equilibrium during large time steps on a linear model. It is possible to use an implicit solver for a dynamic case on a non-linear model, but the solver may not converge to a solution and in best possible situation the solver has to take larger amount of time increments and therefore increase the computational time. Instead, when working with a dynamic problem, an explicit solver is preferable. This is called Abaqus/Explicit in the program. This allows for inertia in the model and the solver solves for dynamic equilibrium for non-linear models. The dynamic case is a high recoil environment containing resulting vibrations [3].

2.2 FEA of bolt models

FEM modeling consists of simplifications and assumptions to optimize the computation and is a method to solve differential equations that are deemed impossible to calculate analytically. Instead an FE mesh is applied to the model and for each element of the mesh, a numerical approximation is calculated with regard to defined material characteristics, loads, boundary conditions and constraints for each respective element [4].

Another simplification is the design of the model. A detailed model with excessive features and faces takes longer to compute than a proportional fundamental shape due to the meshing of the model. A coarse mesh might miss smaller details, but to include every small detail one could use an excessively small mesh that will take longer to compute. Therefore, details such as chamfers, fillets, cuts and extrusions may be simplified or removed completely. An example of this can be seen in figure 1.

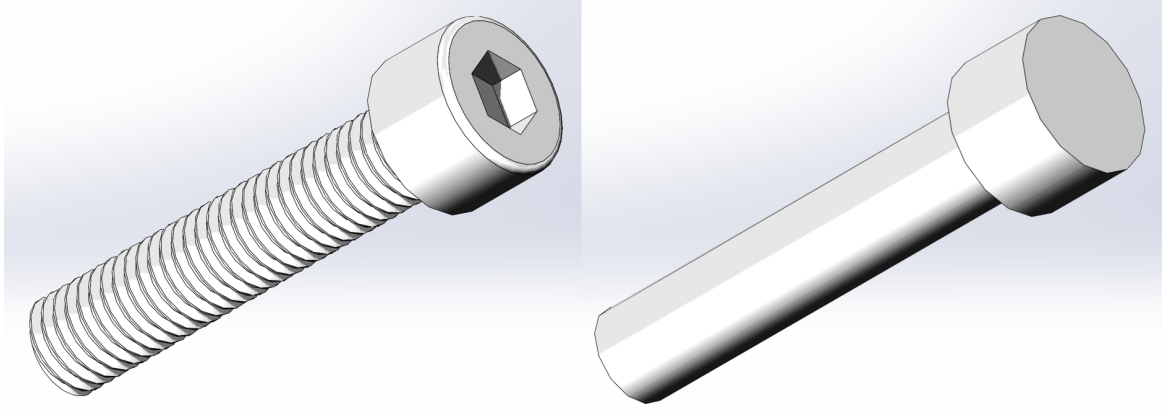


Figure 1: 3D CAD model of a bolt with detailed features (left) and simplified without detailed features (right).

When modeling a system including bolts, the bolts are often removed completely to simplify the process. If one were to include bolts in the model they are usually not modeled as a solid part. As mentioned in the introduction, there are different ways to model a bolt but this report will be limited to three of those methods: coupled, hybrid and solid. Coupled- and solid bolts are commonly known and hybrid bolt is a combination of both and is used at Aimpoint.

A solid bolt is as the name implies, the whole bolt is modeled as it is, as seen in figure 1, and gives a more realistic result compared to the other models. A coupled bolt consists of a wire element for the shaft and nodes for the head and the thread. Compared to the solid bolt, the coupled bolt is the simplest model [5]. The third method is as mentioned a combination of both and is used at Aimpoint. This method creates a realistic model of the contact between the bolt head and the connecting surface, while saving computational time by not having to model the threaded part of the bolt. However, an own interpretation of the hybrid bolt was used to simulate the strain gauge that is to be used during the experiments. If a wire can represent the gauge, then similar behaviors might be able to be computed. This interpretation of the hybrid bolt will be used, and not the one used by Aimpoint.

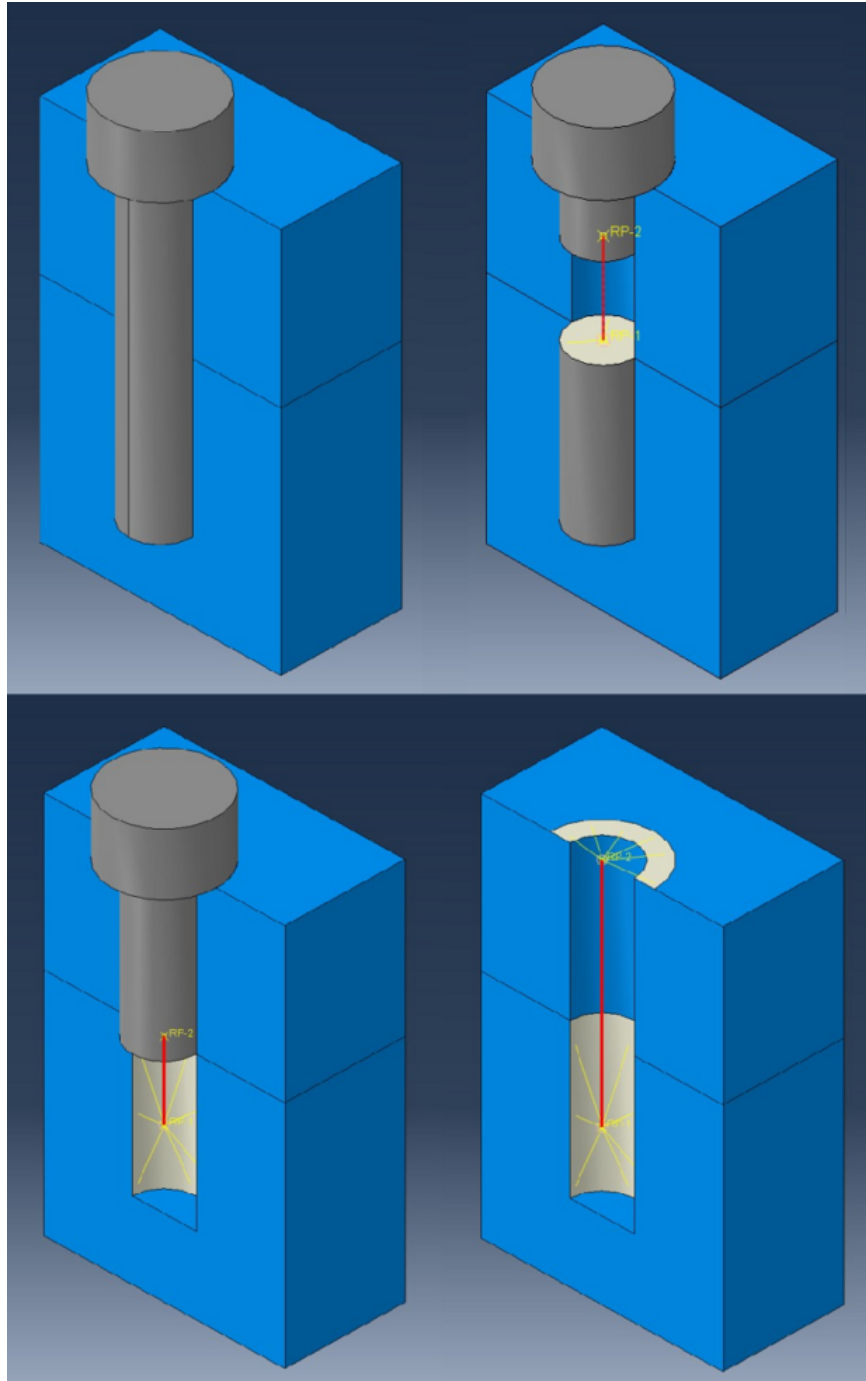


Figure 2: Four different methods on how to model a bolt. A solid bolt (top left), an own interpretation of a hybrid bolt with a coupled wire for a strain gauge (top right), a hybrid bolt used by Aimpoint with a coupled wire instead of the threaded part of the bolt (bottom left), and a coupled wire (bottom right) replacing the head and the threaded part of the bolt. The hybrid bolt in the top right will be the one used in the simulations, and not the one used by Aimpoint in the bottom left.

When using coupled and hybrid bolts, different behaviors can be applied to the

wires. These can result in the model being rigid, act as beam or even act as a spring [6]. The spring behavior will be of interest in this report as it can be used to easily model a clamping force of a bolt since a bolt is stretched similarly to a spring when tightened [7]. One equation to keep in mind when working with springs is

$$F = k * x, \quad (1)$$

where F is the force needed to change the length of the spring by the distance x through extension or compression. The spring stiffness is represented by k .

2.3 Mass scaling

Another optimization aspect to take into consideration is the time step. Similarly to a finer mesh, a smaller time step generates a longer computation as more steps are needed to be analyzed compared to taking larger steps. A stable time step can be described by the following equation [8]:

$$\Delta t \leq \frac{L^e}{c_d}, \quad \text{where } c_d = \sqrt{\frac{E}{\rho}}. \quad (2)$$

In other words, the time step Δt is a function of the length of the smallest element, L^e , and the speed of the stress wave through the material, c_d . The speed of the stress wave is then described by Young's modulus, E , and the density of the material, ρ . Therefore, when getting an unstable time step it can be resolved by increasing the density of the material. However, the increase is not allowed to change the density of the material to such a degree that it becomes a completely different loading case.

2.4 Material characteristics

Material models are fundamental when working in the FEM program Abaqus and below are the different characteristics that will be used in this project. When defining a material, five categories are available: general, mechanical, thermal, electrical/magnetic and other. The first two will be used.

A general characteristic is the material density. The rest of the characteristics will belong to mechanical category, which is then divided into the subcategories, elasticity and plasticity. For elasticity, two values are defined: Young's modulus and Poisson's ratio. Poisson's ratio will be described in the following subsection. Young's modulus is also known as the modulus of elasticity and is the relative stiffness of a material. It is described by the ratio between the uniaxial stress and strain

$$E = \frac{\sigma}{\epsilon}. \quad (3)$$

Notice how this also can be related to Hooke's law for linear elastic materials

$$\sigma = E * \epsilon. \quad (4)$$

Both Young's modulus and Poisson's ratio will in this case be read from material sheets for the materials used in this project. This is also applied for when using the plasticity category, where yield stress is used. The stress values used are the yield stress and the ultimate tensile stress. The yield stress is the point on the stress-strain curve where the material changes from elastic to plastic, while the ultimate tensile stress is the maximum stress the material can withstand before breaking [9]. These are illustrated in figure 3. The corresponding plastic strain for the yield stress is zero and for the ultimate tensile stress it is calculated with

$$\epsilon_{plastic} = \epsilon_{total} - \frac{\sigma_{yield}}{E}, \quad (5)$$

where ϵ_{total} is the total strain, σ_{yield} is the yield stress and E is Young's modulus.

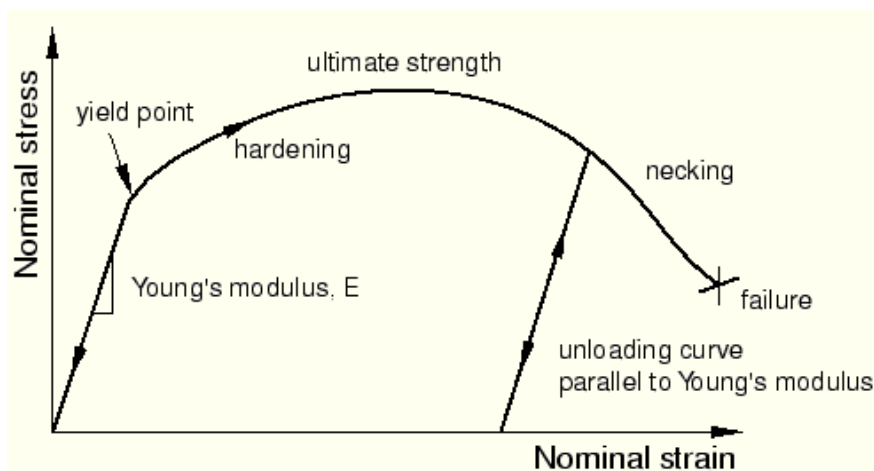


Figure 3: Stress-strain behavior of a material [10].

2.5 Strain gauge

One challenge in this project is to measure the deformation of the bolt for different loads. A strain gauge is used to measure, as the name implies, the strain of a material. The strain gauge is attached to an object and as that object deforms, so does the gauge. The deformation of the strain gauge causes a change in resistance. Use can be made of Poisson's ratio of a material, which is the ratio between transversal strain and longitudinal strain in a material. As seen in figure 4, the transversal direction is represented by the x-axis and the longitudinal direction is represented by the y-axis. Normally, when a material is experiencing tension, the longitudinal dimension is expanded and the transversal dimension is contracted. If the material is instead compressed the result will be opposite [11].

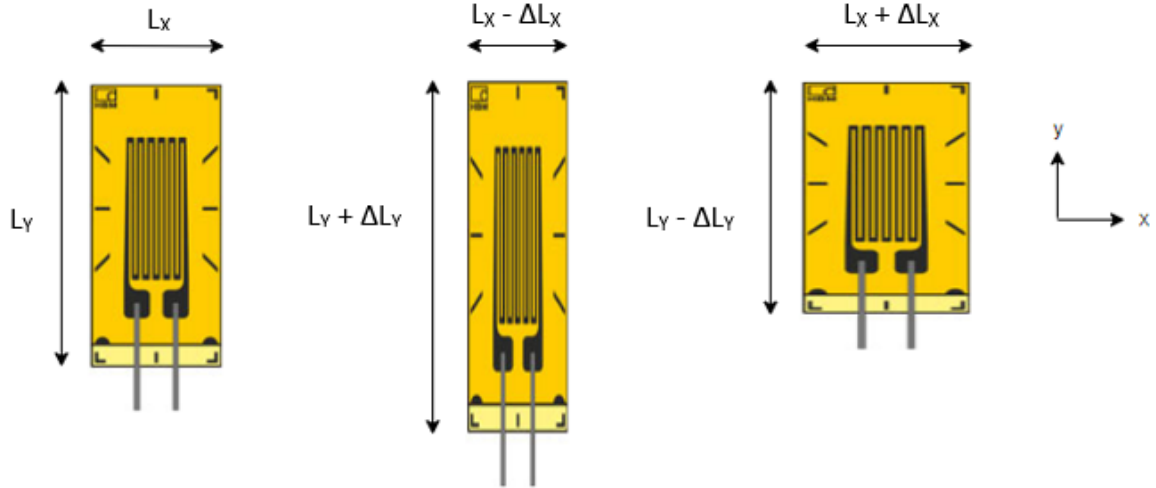


Figure 4: How a strain gauge changes in length when experiencing uniaxial tension (middle) and compression in the y-direction (right). Undeformed strain gauge (left) is defined by the original lengths in both x- and y-direction [12].

Poisson's ratio can be described as

$$\nu_{xy} = -\frac{\epsilon_x}{\epsilon_y}, \quad (6)$$

where the strain is then described as

$$\epsilon_i = \frac{\Delta L_i}{L_i}, \quad (7)$$

which is the change in length after the tension or compression divided by the original length. How this is then applied to a strain gauge is through the pattern of the gauge. When the strain gauge is exposed to tension or compression, the cross section of the gauge's wire decreases or increases which in turn results in an increase or decrease respectively in resistance. Simply put

$$R = \frac{\rho l}{A}, \quad (8)$$

where R is the resistance, ρ is the electrical resistivity of the material, l the length of the conductor and A the cross-sectional area. This shows the proportion between the resistance and the area as described above.

The strain gauge only measures axially and will therefore only read result from the normal strain it is exposed to. Therefore, when subjecting a bolt to shearing in this project, keep in mind that the shearing strain is not measured. This can be seen in figure 5, which is a hyperbolic example.

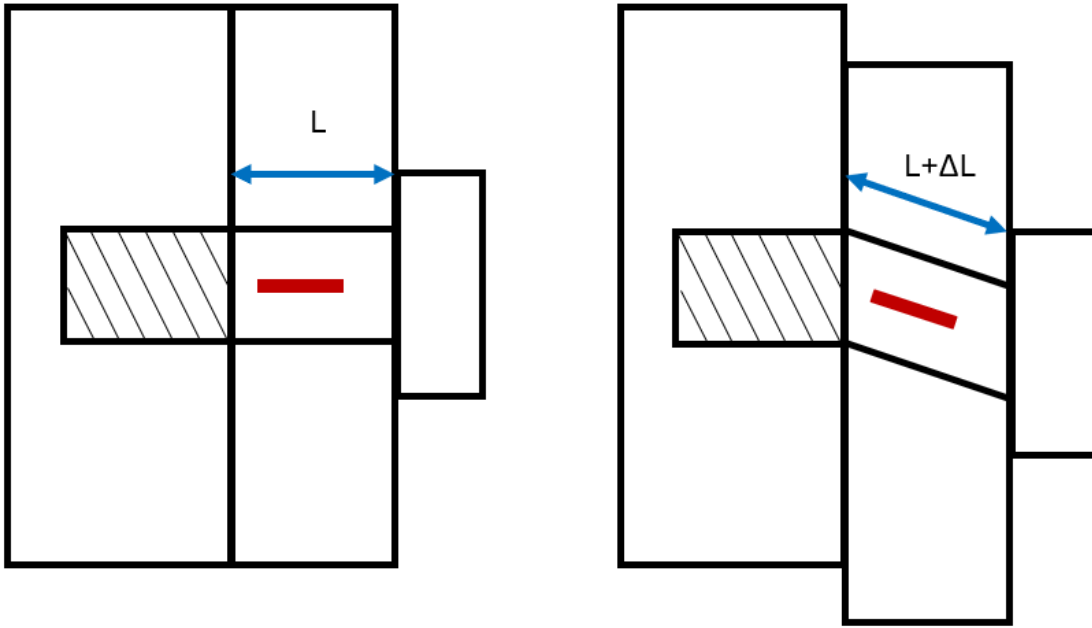


Figure 5: Normal strain in a shearing bolt. An undeformed bolt and strain gauge (red) with original length L (right) and a deformed bolt with a length difference in the normal direction of the strain gauge (left).

2.6 Wheatstone bridge

When measuring the change in resistance, it may be unreliable since the changes are in the order of $m\Omega$ and may disappear in noise [13]. To mitigate this, use was made of a Wheatstone quarter bridge, as seen in figure 11.

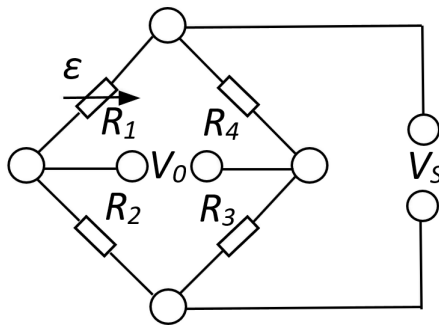


Figure 6: Circuit schematic of a Wheatstone bridge.

A quarter bridge is used in this case due to the use of only one strain gauge which acts as one of the four resistors in the bridge. If one were to use more than one gauge, the bridge can change into half-, diagonal- or full bridge. These options can, in addition to measure strain, be used to measure strain from bending and torsion, and compensate for temperature effects [13].

A Wheatstone bridge is used to measure the relative change in resistance in the strain gauge. In the figure above, R_2 , R_3 , R_4 are fixed resistors, R_1 is the strain gauge, V_S the voltage source and V_0 the output voltage. The bridge is balanced when

$$\frac{R_1}{R_2} = \frac{R_3}{R_4}, \quad (9)$$

which will make the output voltage equal zero. Therefore, a small change in the strain gauge will be noticed in the output voltage [14]. Even better if a signal amplifier is used to increase the order of the change. The output voltage can be expressed as per following [13]:

$$\frac{V_0}{V_S} = \frac{1}{4} \left(\frac{\Delta R_1}{R_1} - \frac{\Delta R_2}{R_2} + \frac{\Delta R_3}{R_3} - \frac{\Delta R_4}{R_4} \right) = \frac{1}{4} \left(\frac{\Delta R_1}{R_1} \right). \quad (10)$$

The last simplification is due to R_1 representing the strain gauge and is the only resistor experiencing change. The equation can then be expressed in terms of strain [13]:

$$\frac{\Delta R_1}{R_1} = G * \epsilon, \quad (11)$$

where G is the gauge factor, which in this case is a given constant. Lastly, the strain is then calculated by the use of the output voltage

$$\epsilon = \frac{4}{G} * \frac{V_0}{V_S}. \quad (12)$$

To determine if the strain measured is reasonable, a last formula can be used as a control. As the cross section area of a sample can be derived and the load is known, the strain can also be calculated as per following:

$$\epsilon = \frac{F}{AE} \quad (13)$$

where F is the load and E the Young's modulus [13].

2.7 Piezoresistive accelerometer

A piezoresistive accelerometer makes use of a strain gauge but on a smaller scale. It consists of a mass supported by springs in which the strain can be measured, the acceleration is then correlated with the strain and mass displacement [14]. One aspect which will be looked at further into the report, is the correlation between the acceleration of the accelerometer and the force is it exerted to. This can be done with the help of Newton's second law

$$F = m * a, \quad (14)$$

where the force F of an object is equal to its mass m multiplied by its acceleration a .

3 Abaqus glossary

For easier reading throughout this report, settings used for this project will be defined in this section. The settings in this glossary will be *italicized* when first mentioned throughout the rest of the report. For more in depth descriptions, please refer to the Abaqus User Manual references at the end.

Amplitude A setting to define a time varying function for an analysis. Amplitude has a list of predefined functions, but there is also the option to create a function from table values. Your defined amplitude can be applied to features such as loads and boundary conditions that are to vary with time. A magnitude of that feature can be prescribed and will be multiplied with the amplitude [15].

Boundary condition Conditions set on the model that define how it interacts to its surroundings or applied forces [16]. Main uses in the project include: locking chosen nodes in desired degrees of freedom (locked in all degrees is called "encastre") and applying acceleration to chosen nodes. Compared to the coupling constraint (see **Constraint - Coupling** below), a boundary condition with encastre will not move throughout the whole simulation, while the constraint will not move in regards to its attached reference point [17].

Connector Defines the connection between two nodes and is built up of three parts: a geometry, a section and an assignment [18].

Connector geometry - Wire A line connecting two nodes. A wire is needed to be able to assign a connector section [18]. See the red line in figure 9 below.

Connector section - Translator Two nodes connected that may move in only one degree of freedom in regards to each other, all other degrees are locked. This can be compared to a bicycle pump that is fixed to the ground or the wall. A connector section can have behavior options applied to be able to act similarly to a material, a spring, a rigid body [19].

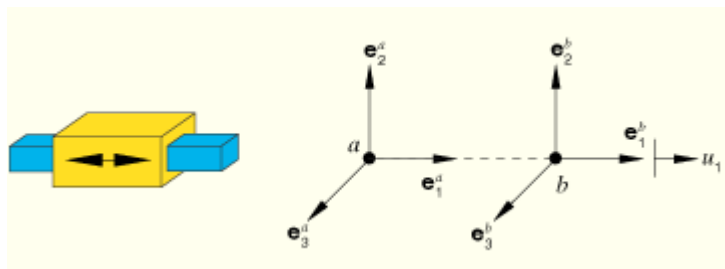


Figure 7: How the connection section called translator works. Two nodes connected that may move in only one degree of freedom in regards to each other [20].

Connector section - Axial Works similarly to the translator that it looks at the relative displacement between the nodes in the axial direction, but the nodes are

free in all degrees of freedom. A connector section can have behavior options applied to be able to act similarly to a material, a spring or a rigid body [18].

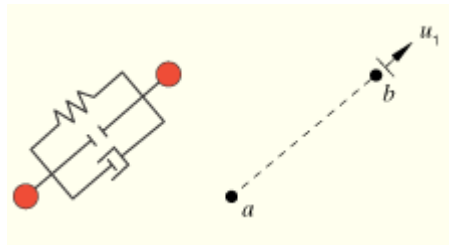


Figure 8: How the connection section called axial works. Looks at the relative displacement between the nodes in the axial direction, but the nodes are free in all degrees of freedom [20].

Connector assignment Assign wires with the desired connector section(s).

Constraint - Coupling A form of rule on how nodes within a chosen surface behaves in regards to a reference point. Any conditions or loads applied to the reference point acts on the whole surface uniformly [5]. In figure 9, the ends of the red wire each have a reference point. They are connected to the white surfaces surrounding them, which can be seen by the thin yellow lines that connect the points to the surfaces.

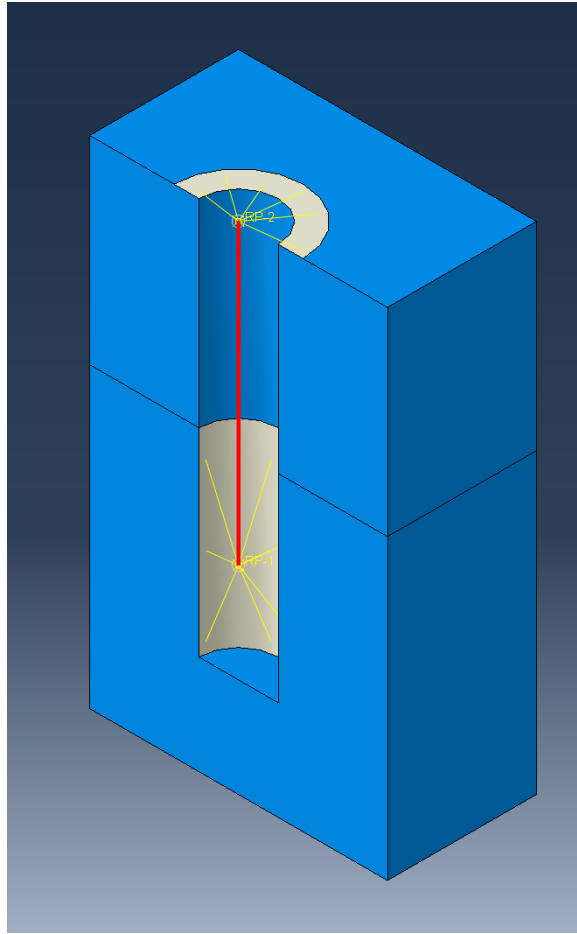


Figure 9: A model of a coupled bolt, halved to see the inside. The white surfaces are the coupled to the yellow reference points RP-1 and RP-2. Yellow arms go out from the reference point to the matching surfaces. The reference points are connected by a red wire that has been assigned a connector section.

Constraint - Tie A tie between two surfaces acts as if superglued together, they are locked to each other throughout the simulation [17]. This is useful when working with bolts since it is not cost efficient to model threads. Instead, a tie between the threaded part of the screw and the hole can be made.

Interaction - General contact A general contact is used to easier set a property for all surfaces that interact or will interact with each other [17]. Interaction properties are then applied to the general contact, see below.

Interaction property Defines how surfaces should interact [15]. There are mechanical, thermal and electrical properties. For this project, only two mechanical properties were chosen: tangential and normal behavior. The tangential behavior between two surfaces is friction and the normal behavior is a form of constraint to make sure that the surfaces cannot pass through each other. This is called a hard contact.

Mesh A global seeding size of the mesh is chosen in which the program will apply it in the best possible way [15]. In this project, the mesh controls are set to tetrahedral elements of quadratic order. Tetrahedral elements are three dimensional. Linear elements have nodes in each corner while quadratic also have nodes midway between two corner nodes.

Step A simulation consist of one or more steps. For each step, a time period and time increment size is defined. Settings such as those mentioned above can be created, propagated or disabled depending on which order of action is desired [17].

4 Method

The project consists of a quasi-static study followed by a dynamic study. As mentioned earlier, the quasi-static study is divided into two parts. The first part is to test a general linear strain gauge in the tensile machine, as it is the most common strain gauge, and the second part is to conduct the same test but with a strain gauge embedded into a bolt. This type of gauge is special and not commonly used and therefore will be compared to the general linear gauge. The same type of bolt is then to be used in the dynamic test. Since the methods are the same for both studies, they are described together. However, keep in mind that they were completed one by one on different occasions. The aim of the quasi-static study is to confirm that the strain gauges are reliable measuring devices for the dynamic tests. The dynamic study will then answer the project's questions: is it a reliable measurement technique and can the results help with developing a reliable FEM model of fasteners in a similar environment? In order to complete the project, the order of operation needed to be as following for both parts:

1. Make 3D models of samples and fixtures.
2. Initial FEM analysis.
3. Manufacturing of fixtures and preparation for tests.
4. Perform tests.
5. Analyze test data.
6. FEM verification (only for dynamic test).

In the following text, each step of the methodology is described by how they were done and with what type of equipment used to complete the task. All equipment was provided by Aimpoint and used at their headquarters in Malmö. Aimpoint also provided in-house manufacturing of 3D models and an electrical lab.

4.1 3D modeling

The 3D models were to be made in the program called SolidWorks. Requirements when creating the 3D models of the fixtures where:

1. The strain gauges have to fit in or on the fixture. The fasteners used for the different machines can be seen in figure 10 below.
2. The fixture has to be fitted to the fasteners of the machines used for the tests.
3. Specifically for the dynamic test, the fixture could not exceed the weight limit of 10kg.

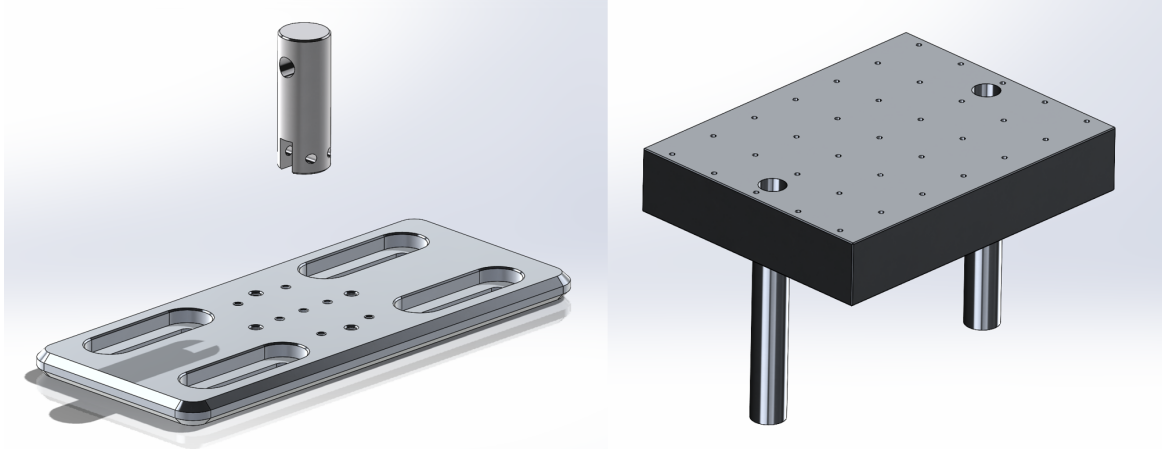


Figure 10: The fasteners that the modeled fixtures have to fit in. A fastener for the tensile tester MTS Criterion 43 (left) and a fastener for the shock machine Elstar (right). 3D models provided by Aimpoint.

4.2 Initial FEM simulations

Initial FEM simulations were made to evaluate the design of the 3D models of the fixtures and make sure that they could withstand the forces of the tests. The program Abaqus CAE was used for this step and contains many complex settings and features. Those used for this project will be *italicized* and are referred to in the Abaqus glossary.

4.2.1 Quasi-static simulation

Due to the test being quasi-static, these simulations were made as implicit. All 3D parts were imported and each were assigned a material, *mesh* and features which will be in more detail below and in the glossary. The fixtures were assigned aluminum and for the model with the strain gauge embedded bolt, steel was used for the bolt. Tables 1 and 2 contain the material properties used in the simulations. When applying the material, the whole part is set as solid and homogeneous.

Aluminum	
Property	Value
Density	2,7 g/cm ³
Young's modulus	68,9 GPa
Poisson's ratio	0,33
Yield tensile strength Plastic strain	0,276 GPa 0
Ultimate tensile strength Plastic strain	0,310 GPa 0,096

Table 1: Properties of aluminum 6082 used in the FEM simulation [21] [22].

Steel	
Property	Value
Density	7,85 g/cm ³
Young's modulus	210 GPa
Poisson's ratio	0,29
Yield tensile strength Plastic strain	0,8 GPa 0
Ultimate tensile strength Plastic strain	0,965 GPa 0,175

Table 2: Properties of steel used in the FEM simulation [23].

To reduce the number of parts to be analyzed, though it may seem contradictory to the project, all pins and bolts to hold the fixture in the machine were excluded. Instead, use was made of *coupling constraints* to mimic stiff cylindrical beams through the holes. For the second model where the bolt is included, a *tie constraint* was set on the threaded surfaces of the hole and the bolt. Moving on, an *encastre boundary conditions* was set to the bottom of the fixture, since it is how it is fastened in the machine. The model was designed to be held in the machine by pins and therefore a load of 5000N was applied to the reference points of the coupling constraints subjected to the pulling force.

In addition to loads and conditions, *interactions* needed to be defined. A *general contact* was set with *tangential and normal properties*. The tangential property (friction) was set to 0.3 and the normal property was set as hard contact. Further, there is only one *step* in these simulations. It only takes one time step that lasts one second. This allows the mesh to be finer without costing too much in computational time. All settings are created and used in this step. The results are then shown as stresses throughout the fixture to see if it is able to withstand the pulling forces of the tests.

4.2.2 Dynamic simulation

This simulation is done as explicit as the test is dynamic. The bolts needed to be modeled since they are to be analyzed later on. When modeling the bolts, inspiration was taken from past simulations done at Aimpoint and was used as a learning opportunity on how to use Abaqus. In those simulations a hybrid bolt was used, but in order to make this simulation more efficient it was simplified into a coupled bolt. The goal now is only to verify that the fixture will not break during the shock tests, the other bolt models will be analyzed in the verification simulation. Both the coupled- and the hybrid bolt is modeled by using coupling constraints and a *connector*. Therefore, the settings in one of Aimpoint's past simulations could serve as a base. Moving on, a *translator* was used as the *connector section*. No behaviors were set on the translator, these will instead be altered in the verification simulations. Lastly, the wires were assigned the same translator sections through *connector assignment*.

This simulation consists of two steps: tightening of bolts and recoil of fixture. To not overcomplicate the first step, since the recoil test is the main part of this project, a clamping force of 1500N was used. For each node in the connector, a load was applied in opposite directions to each other. To be able to keep the bolt tightened

during the recoil, the nodes were locked in their tightened position ("Hold bolts"). The boundary conditions vary for each of the steps and for an easier overview see table 3. In the first step, the table of the machine is encastred as to not move when the bolts are tightened ("Ground"). For the second step, the recoil is set as an acceleration boundary condition ("Recoil") and the encastre is unlocked only in the same degree of freedom as the recoil ("Level while recoil"). As can be seen in the 3D model in figure 10, the legs of the table are what is used to direct the recoil and since they don't allow the table to move in any other direction than up and down, the same will be applied in the simulation. By using the *amplitude* setting, the recoil is defined as a half sine wave with a duration of 0,5ms and an wave amplitude of 1 with a line on zero for 0,5ms to allow effects after the recoil to be recorded. The acceleration is then set to 400G and is applied to the sine wave. Both steps have a time period of 1ms and have 50 time intervals each. A mass scaling with a target time increment of 1E-8, where the element mass will be scaled if the time step is below the target.

Name of BC / Step	Tightening	Recoil
Ground	Created	Deactivated
Hold bolts		Created
Level while recoil		Created
Recoil		Created

Table 3: The different steps of the dynamic explicit simulation and the corresponding boundary conditions that are created and deactivated during the different steps.

4.3 Preparations

When the simulations were verified, the models were sent for manufacturing. In the meantime, preparations were made for the tests. These include: order strain gauges and glue, prepare bolts for both tests, solder a Wheatstone bridge, connectors and cables, and make sure that the sampling system receives correct signals. The preparation of the bolts include drilling holes into the top of the bolts where the strain gauges are then inserted, glued in place and then cured. The strain gauges were ordered from HBK (Hottinger Brüel & Kjær) and their characteristics can be seen in table 4.

Type	Measurements [mm]	Resistance [Ω]
Linear gauge, 1-LY1x-10/120	10×4,6	120
Cylindrical gauge, 1-LB11-3/120ZW	11,5×2 \emptyset	120

Table 4: A linear strain gauge [24] and a cylindrical strain gauge [25] from HBK (Hottinger Brüel & Kjær) used throughout the project and their respective measurements and resistance.

Starting with the quasi-static study, the preparation consisted of soldering a Wheatstone bridge, as seen in figure 11, to be able to get a clear voltage output when the

strain gauge is engaged. Each resistor has a resistance of 120Ω . The Wheatstone bridge will then be connected to a voltage supply and a multimeter.

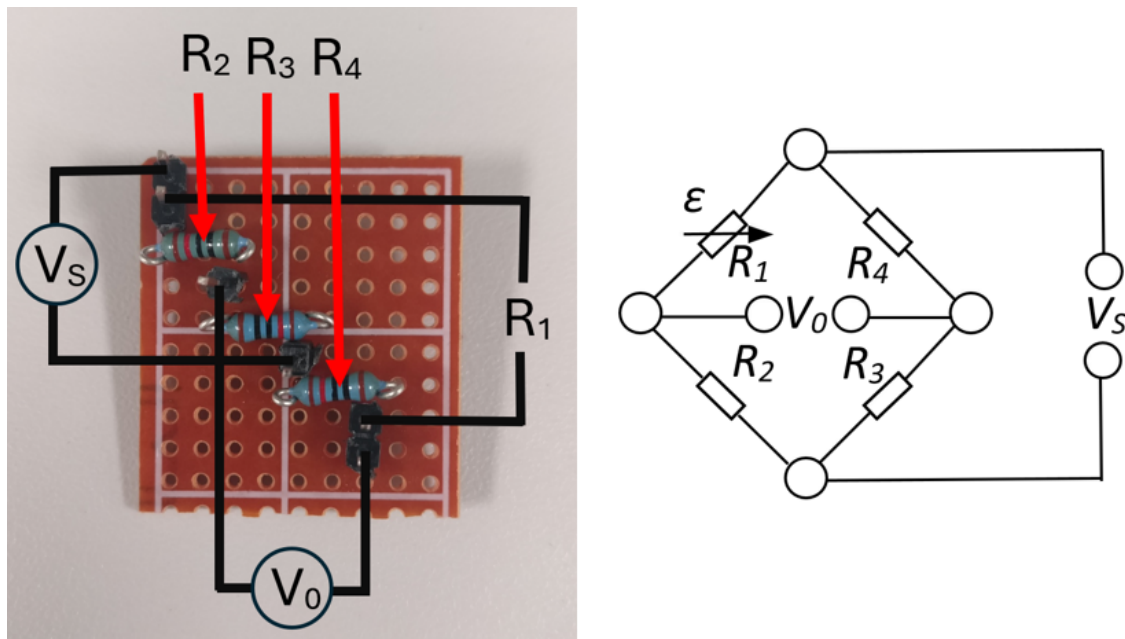


Figure 11: Soldered Wheatstone bridge (left) compared to the schematic of the theoretical Wheatstone bridge (right).

The linear strain gauge could not be glued onto the fixture until after it was manufactured. For the cylindrical gauge in both studies, the bolts could be prepared separately and does not require the fixture to be manufactured. A hole with a diameter of 2mm had to be drilled from the top of the bolt, followed by inserting and gluing the strain gauge in the hole. The glue had to cure in an oven in 60°C for 3 hours. The copper threads sticking out of the bolt head had to be connected to a wire which in turn will be connected to the Wheatstone bridge in the quasi-static test and a connector in the dynamic test. The bolt preparation can be followed in the picture series below, figure 12 and 13.

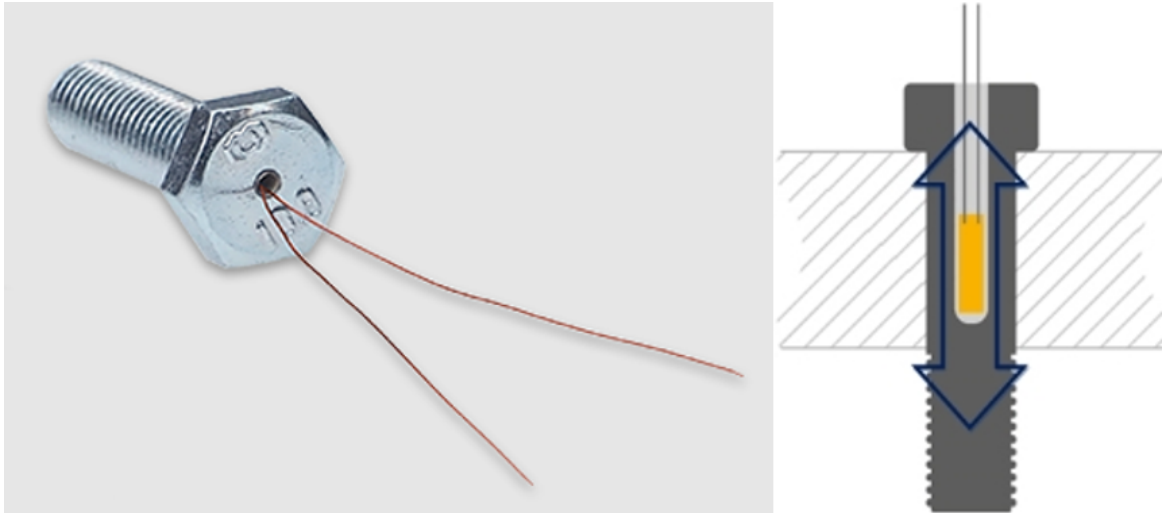


Figure 12: A prepared bolt with a drilled hole and glued strain gauge as seen in the data sheet from HBK (left) and a cross section of a bolt with an assembled gauge (right) [25].

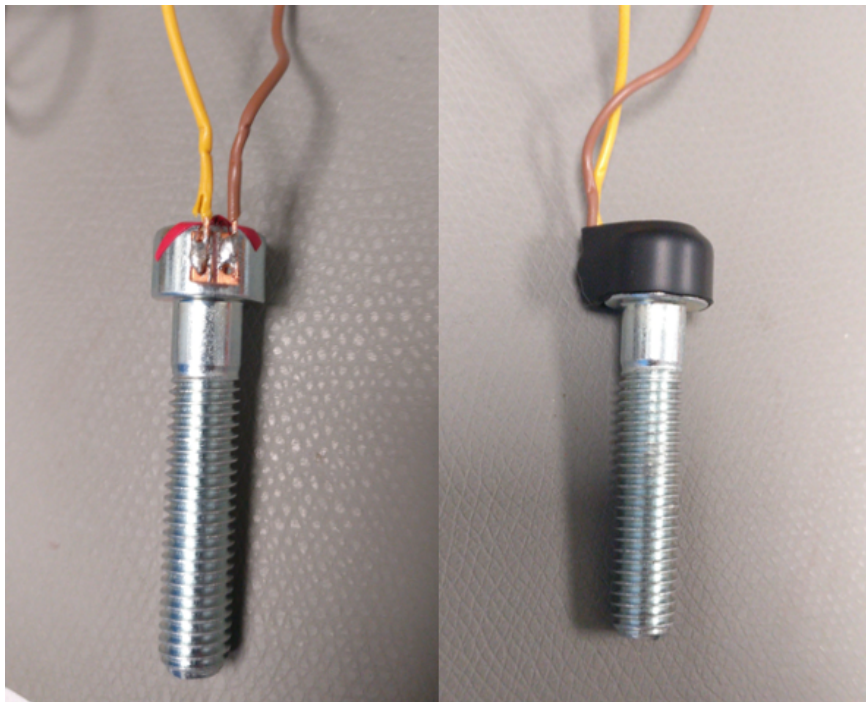


Figure 13: One of the bolts used for the tests with soldered threads and cables (left), covered with a protective heat shrinking tube (right).

The cables from the bolt in the dynamic test needed to be soldered to a connector that fits the sampling system SIRIUSi-HS. The sampling system is from DEWESoft and comes with a software for data acquisition. DEWESoft's training manual for strain measurements include a schematic on how to connect a strain gauge to a connector

to be able to have a built-in Wheatstone bridge in the system. The schematic can be seen in figure 14 and the connector in figure 15 which is soldered according to the schematic.

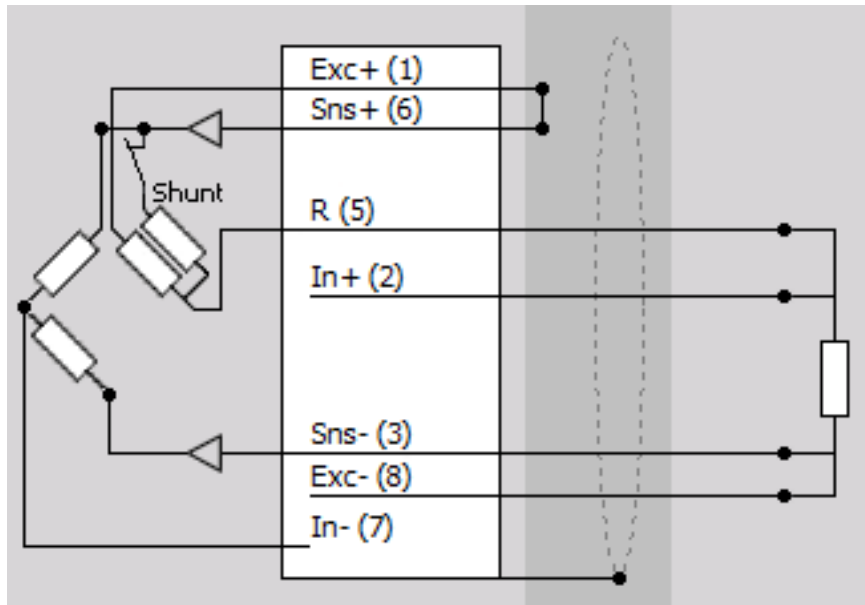


Figure 14: From right to left of how to solder a connector to have a built in 4-wire quarter-bridge in the sampling system SIRIUSi-HS: a single resistor representing the strain gauge with four wires going into the the connector pins, a large white box in the middle containing the pin numbers and what they represent, and the quarter Wheatstone bridge which is built into the sampling system [26].

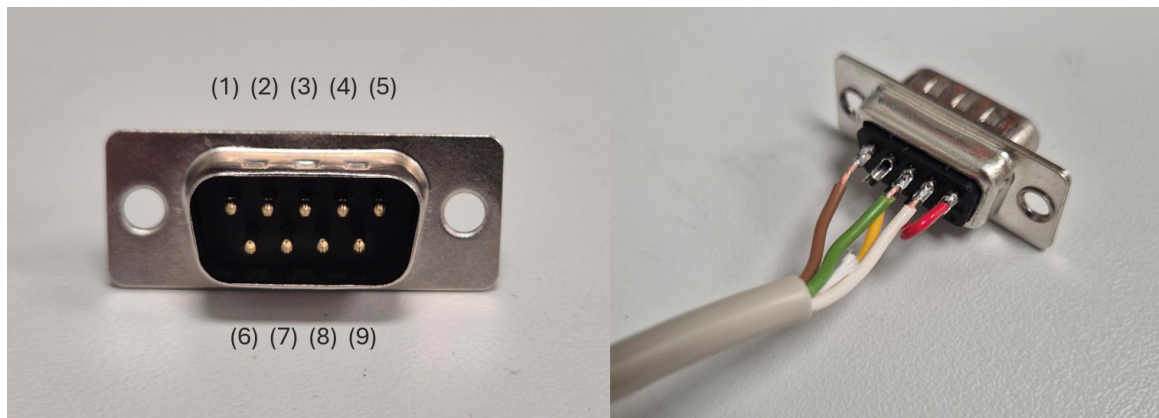


Figure 15: A connector (left) and how it was soldered to be able to get a quarter Wheatstone bridge in the sampling system SIRIUSi-HS (right). The numbers are labels for the pins and are represented in the schematic in figure 14.

Before conducting the tests, all equipment was inspected: made sure that all solders gave a connection, the strain gauges gave a signal and the sampling systems

received and plotted correct signals. This was done simply by trying to compress, pull and hit the fixtures to see how the signal reacted.

4.4 Tests

The first test is a quasi-static tensile test which uses the MTS Criterion 43 tensile machine seen in figure 16. A multimeter and a voltage supply was used in combination with the prepared Wheatstone bridge and cables, see figure 17. For each test, the pulling rate was set to 0.1mm/min and a trigger was set to stop the machine when the desired maximum force had been reached. Eight tests were conducted for each of the strain gauges, ranging from 500N to 5000N with increments of 500N until 3000N and then increments of 1000N for the last tests. See table 5 for the test sequence. The voltage was set to 5V after testing that different voltages did not affect the result.

Test	Force [N]
1	500
2	1000
3	1500
4	2000
5	2500
6	3000
7	4000
8	5000

Table 5: Number of tests and the corresponding pulling force in the tensile machine MTS Criterion 45.



Figure 16: The tensile tester MTS Criterion 43.

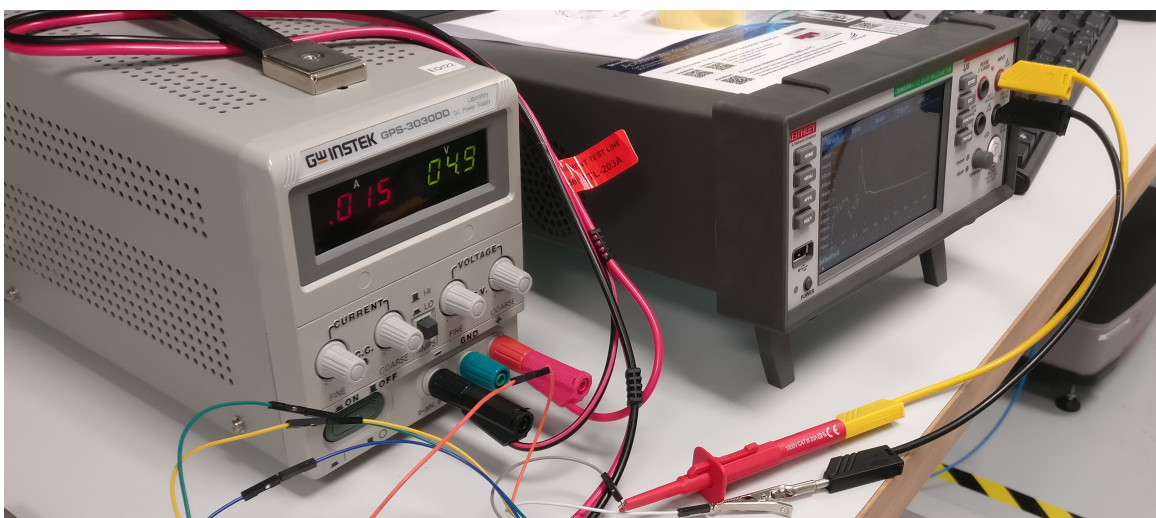


Figure 17: Voltage supply (left) and multimeter (right).

The second test was the dynamic test in the shock machine Elstar. Other equipment needed for this, was the sampling system SIRIUSi-HS, accelerometers, the prepared bolts, cables and connectors, as can be seen in the figures 18 and 19 below. The fixture and the bolts had to be screwed in place, where the bolts were tightened with a moment of 4,5Nm and 5Nm. The different moments are due to the use of different tools since the same tool did not fit when mounting the fixture into the machine. The two moments are the minimum moment available on each tool. Next, the accelerometers were mounted. One was linked to the computer of the machine which was mounted in the "table" of the shock machine, see the rightmost white cable in figure 18. The other one was mounted on the middle weight of the fixture (black cable attached with duct tape) and was linked to SIRIUSi-HS. This was to make sure that both accelerometers show similar results and to be able to translate both the strain and acceleration to force and compare both results.



Figure 18: The shock machine Elstar from the outside (left) and on the inside (right). The black duct taped cable leading to the middle weight is the accelerometer for the fixture, while the rightmost white cable connected to the "table" is the accelerometer for the machine. Grey cables goes into the weights in the middle and the left, which lead to the bolts.



Figure 19: SIRIUSi-HS with the accelerometer in the first channel and the two bolts to be analyzed connected to a channel each, the third and the fourth.

The machine is controlled by inputting the height of the table. Depending on the height and which dampeners are used (the four black circle pads in fig 18), it will result in different recoils. The black pads are default and only the height was a contributing factor in this test.

An initial test was conducted to make sure that everything worked as intended, which was then followed by a test series. Each test consisted of three shocks of the same height. If successful, the height would be increased for the next test consisting of three shocks. Before each test, the signal is zeroed for easier reading. Table 6 shows the different heights used for each test.

Test	Height [mm]
Initial control (1 shock)	275
#1 (3 shocks)	275
#2 (3 shocks)	325
#3 (3 shocks)	400

Table 6: Height input for the different tests with the shock machine.

Strain and acceleration graphs was provided via the program DEWESoft which receives a signal from SIRIUSi-HS. Due to signal problems before the tests, no strain measurements were taken during the tightening of the bolts. This was done afterwards and then added to the strain data from the recoils.

4.5 FEM verification of recoil test

One of the aims of this project was to verify that FEM-modeling can be used to model bolts exposed to high recoils. Therefore, the experiments were replicated as close as possible in Abaqus and the bolts were modeled according to three different methods: coupled-, hybrid- and solid bolt. When creating simulations for the three

bolt models, all models have a similar base settings as to those mentioned in the initial simulation but differentiate in how the bolt is modeled. The major changes first focus on the structure of the bolt and loads applied, e.g how the connector is defined and the conditions of the tightening step. After finding a fitting connector, more detailed settings are explored such as mass scaling and damping to see if the whole model is dependent on either of these.

For both the coupled bolt and the hybrid bolt a wire is used between the coupled nodes. In the initial simulation they were first set as a translator. The other available option in the long list of connectors was one called *axial*. As mentioned earlier, no behavior were set to the translator. Here, the behaviors analyzed were elasticity, damping and reference length. These behaviors can be compared to a spring and Hooke's law where in the elasticity behavior a stiffness is set and the reference length is based on the displacement. With equations (1), (7) and (13) the stiffness can be calculated:

$$\frac{F}{AE} = \frac{\Delta L}{L} \Rightarrow F = \Delta L \left(\frac{EA}{L} \right) = \Delta L * k$$

$$k = \frac{EA}{L} = \frac{200000 * 36,6}{33,7125} = 217130 \text{ N/mm}$$

where L is the length between the two nodes in the connector. The reference length is then used to contract the length of the bolt until the desired clamping force is reached. The strain measurements from the tightening during the test was used and translated to a force. The bolt tightened with a moment of 4,5Nm gave a strain of 341E-6 and a moment of 5Nm gave a strain of 410,26E-6. With the use of equation (13), these can be written as a force instead which results in 2496N and 3003N. With this information and the same equations as above, the reference lengths for the different bolts were:

$$\Delta L = \frac{F}{k} = \frac{LF}{EA} \Rightarrow \Delta L_{4,5Nm} = 0,0115mm$$

$$\Delta L_{5Nm} = 0,0138mm$$

$$L_{ref} = L - \Delta L \Rightarrow L_{ref_{4,5Nm}} = 33,7010mm$$

$$L_{ref_{5Nm}} = 33,6987mm.$$

With the use of the axial connector with the behaviors above, there is no need for a tightening load on the connector since the reference length takes care of it automatically throughout the whole recoil. With this change, the recoil curve was altered to allow everything to happen in that single step. A line on zero for 0,5ms before the recoil to allow the reference length to take effect before the recoil. Other settings such as damping and mass scaling where changed to see if they had an effect on the overall performance.

When working with the whole 3D model of the bolt, there is no need to define a connector or behaviors. It is simply a solid bolt with the material parameters that

are assigned to it. The difficult part is to tighten the bolt. An attempt was made to set the steel of the bolt to an orthotropic material and shrink the bolt in only one direction with the help of temperature. In the end, to save time, the decision was made to not include the tightening of the bolt and do as during the tests and add the tightening strain to the recoil data. Another problem with using a solid bolt is how the data is recorded. A connector in a coupled bolt can record the force in similar terms to how the strain was translated to force above, while if a connector is embedded into the solid bolt the displacement of the wire is recorded. This can also be translated into force by using the strain equations (7) and (13).

5 Results - Quasi-static study

5.1 3D modeling

The requirement for the 3D modeling was that the strain gauges had to fit onto the model and in turn, the models were to fit in the existing fasteners of the machines. In addition, the model for the recoil test was not to exceed the weight limit of 10kg. The results of the 3D modeling can be found in figures 20 and 21 below.

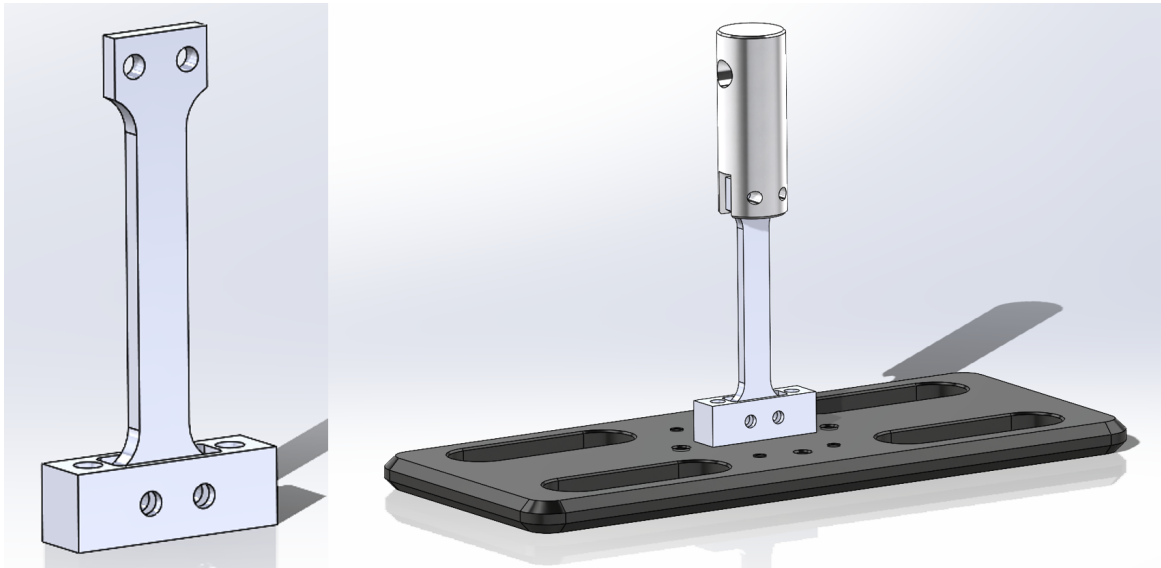


Figure 20: 3D model of fixture for testing a linear strain gauge (left) mounted into the fasteners of the tensile tester MTS Criterion 43 (right).

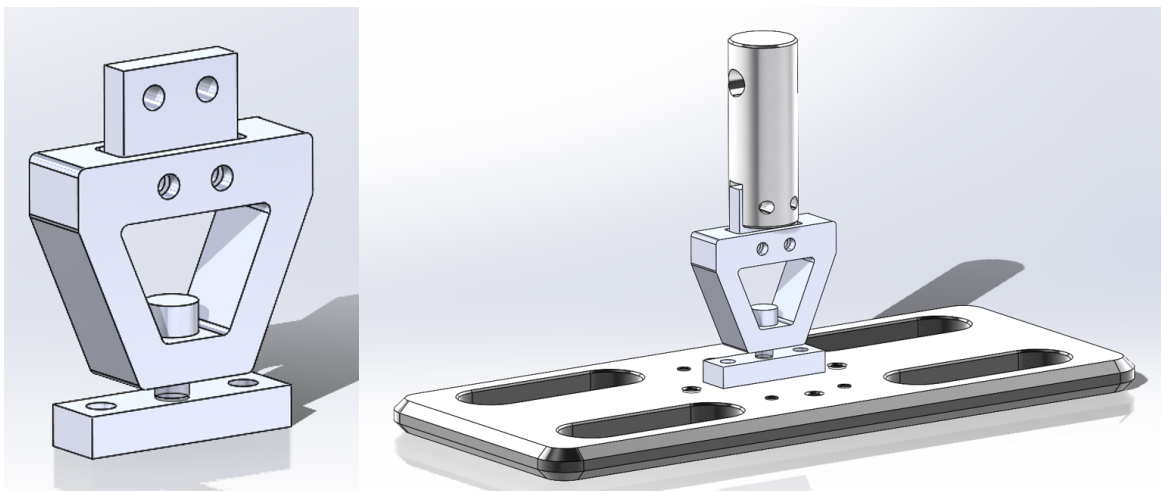


Figure 21: 3D model of fixture for testing a bolt strain gauge (left) mounted into the fasteners of the tensile tester MTS Criterion 43 (right).

5.2 Initial FEM simulation

Initial FEM simulations were made to evaluate the design of the 3D models of the fixtures and make sure that they could withstand the forces of the tests. Figure 22 and 23 show the stresses throughout the fixtures when they are subjected to a pulling force of 5000N. The deformation of the fixtures are scaled to be exaggerated to show how it behaves. The first fixture experiences a maximum stress of 109,2MPa and the second fixture experiences a maximum stress of 184,7MPa which is below the limit for plastic deformation for the aluminum alloy used.

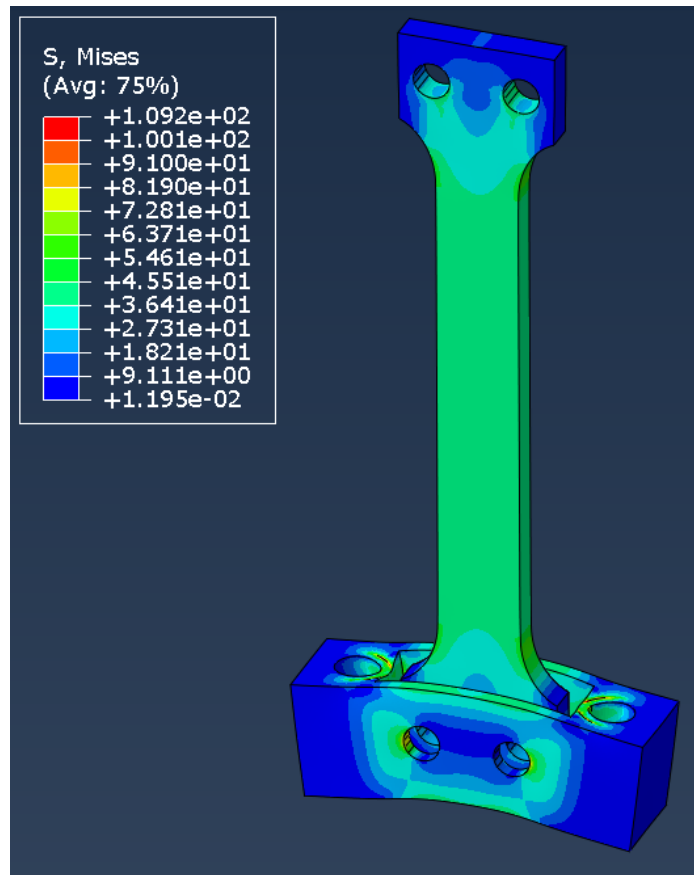


Figure 22: FEM simulation replicating the tensile test with a force of 5000N, resulting in stresses throughout the fixture represented by a color scale. The maximum stress is recorded to 109,2MPa.

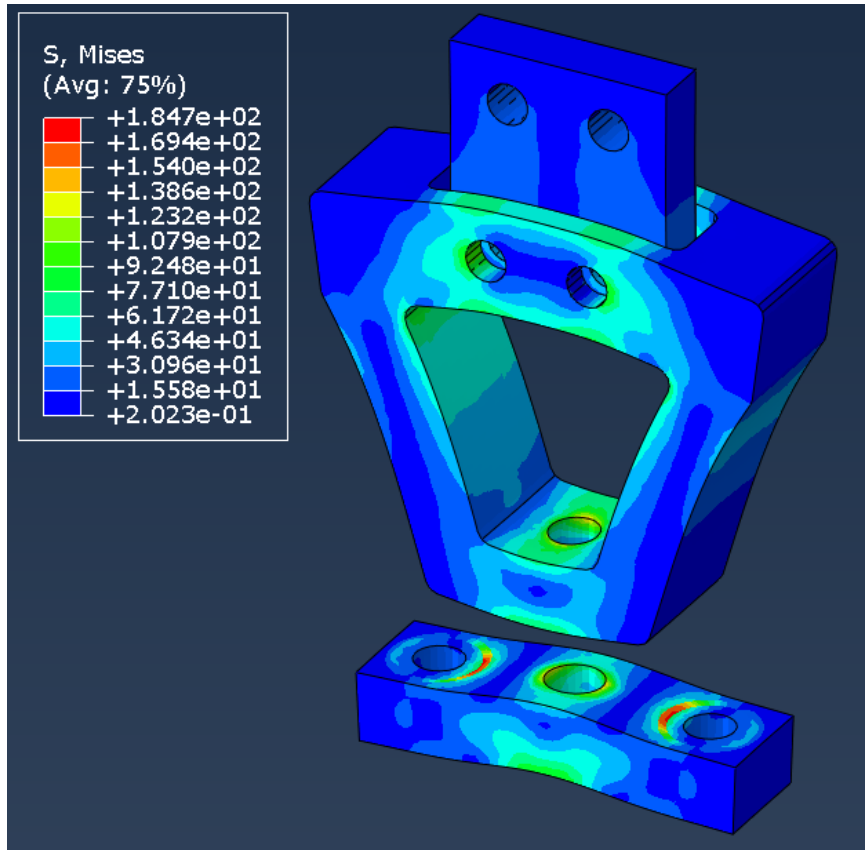


Figure 23: FEM simulation replicating the tensile test with a force of 5000N, resulting in stresses throughout the fixture represented by a color scale. The maximum stress is recorded to 184,7MPa.

5.3 Tests

Eight tests were conducted for each of the strain gauges, ranging from 500N to 5000N with increments of 500N until 3000N and then increments of 1000N for the last tests, as according to 5. The pulling rate was set to 0.1mm/min and a trigger was set to stop the machine when the desired maximum force had been reached. The last test for both fixtures can be seen in figure 24 and the rest of the graphs from this test can be found in the appendix in figure 41 and 42.

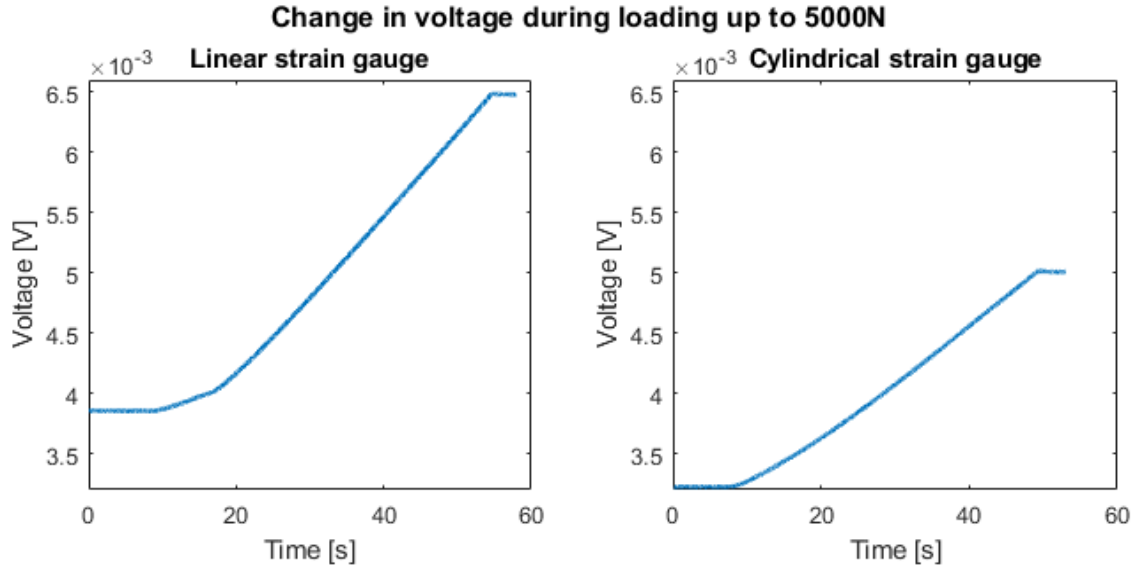


Figure 24: Voltage measurement during a quasi-static loading of 5000N of a linear strain gauge and a cylindrical strain gauge.

As mentioned earlier, the signals of the strain gauges were validated by comparing them to the theoretical values using equations (12) and (13), and the values $G = 2,05$, $V_S = 5V$, $E = 200GPa$, $A_{linear} = 70mm^2$, $A_{cylindrical} = 36,6mm^2$ and F is the different loading cases between 500N to 5000N. For the exact values used for V_0 and the resulting strain ϵ in the graphs of figure 25, please see tables 9-12 in the appendix.

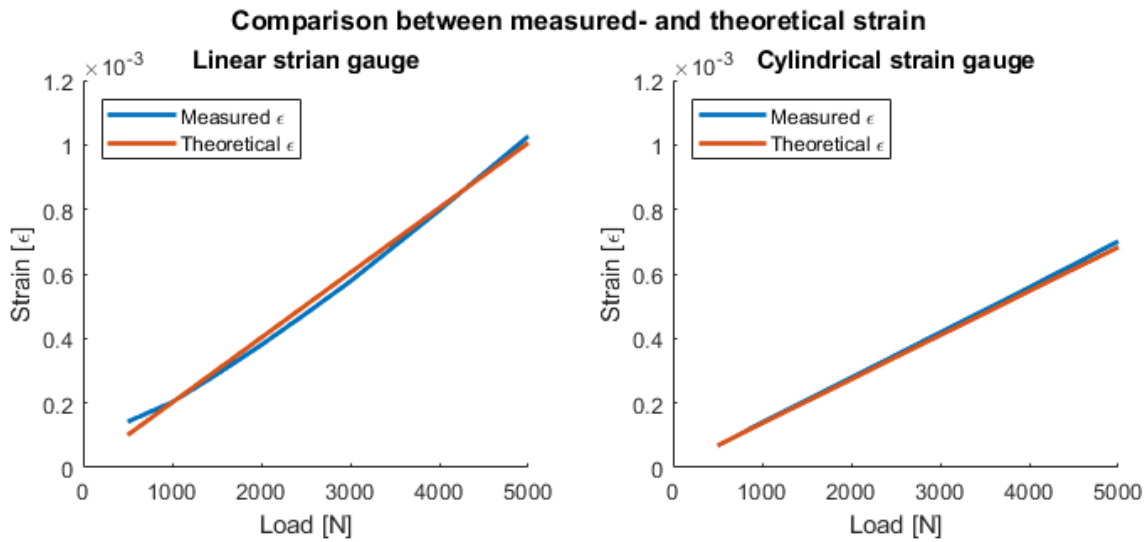


Figure 25: Strain measured with difference in output voltage. Blue line is the strain measured and calculated from the test, the orange line is the strain calculated from the verification equation.

6 Results - Dynamic study

6.1 3D modeling

The requirement for the 3D modeling was that the strain gauges had to fit into the bolts and the models were to fit in the existing fasteners of the machines. In addition, the model for the recoil test was not to exceed the weight limit of 10kg. The results of the 3D modeling can be found in figure 26 below. The resulting weights of the different parts were: 1,391kg for each round weight on the sides, 2,236kg for the middle weight and 3,897kg for the fixture. The total weight is therefore 8,915kg.

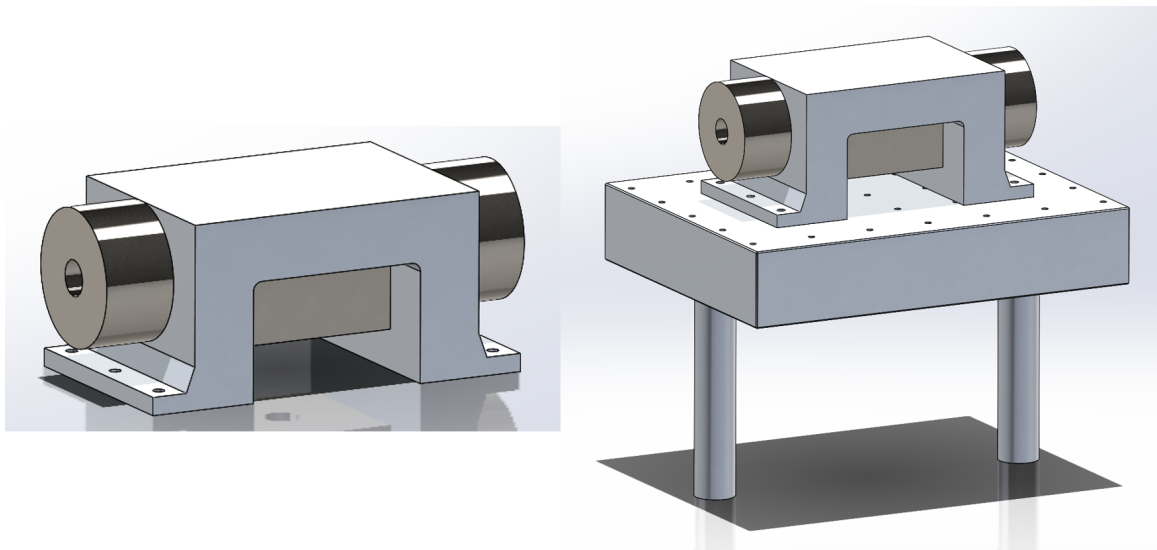


Figure 26: 3D model of fixture for testing normal and shear strain in bolts (left) mounted onto the fastener of the shock machine Elstar (right).

The bolts are placed according to figure 27. The left and right bolt will be perpendicular to the recoil and the bolt in the middle will be normal to the recoil.

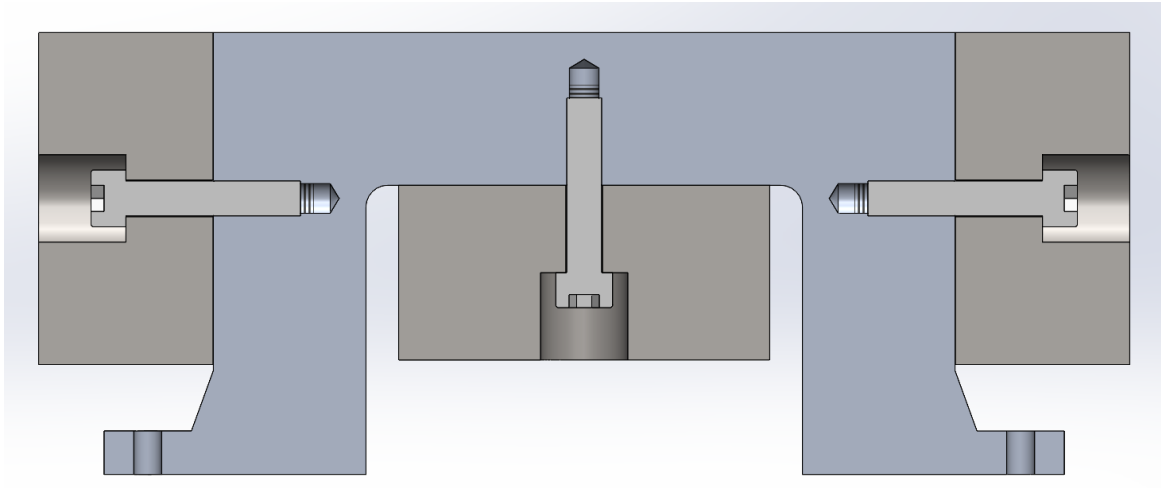


Figure 27: A cut view of the fixture to show the position of the bolts. The left and right bolt will be perpendicular to the recoil and the bolt in the middle will be normal to the recoil.

6.2 Initial FEM simulation

Compared to the quasi-static case, the fixture is built to withstand high recoils better than the bolt, since the bolts are the test subject. The results in figure 28 show that the fixture will not break before the bolts and that the stresses are concentrated in and around the holes for the bolts.

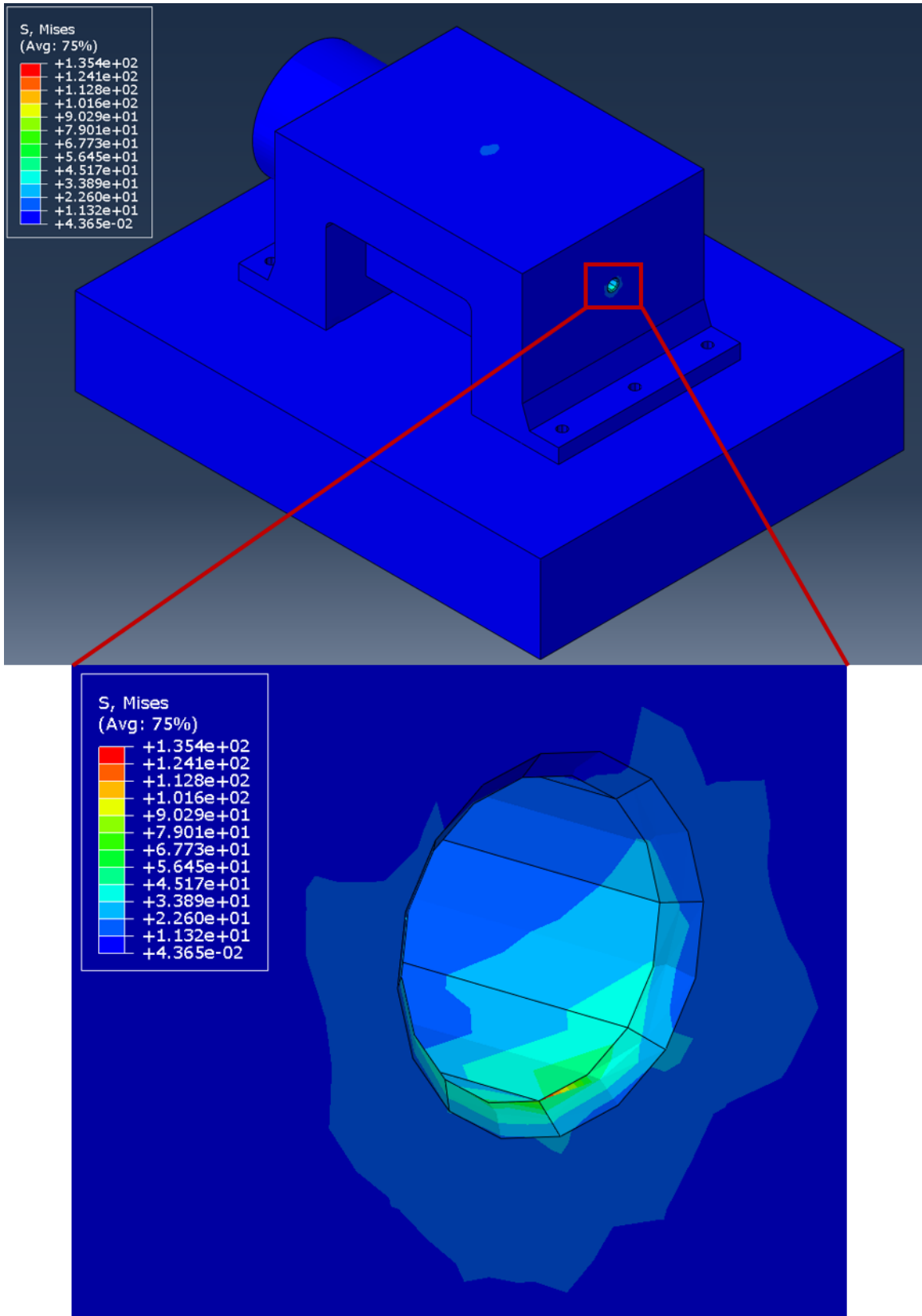


Figure 28: FEM simulation replicating the shock test with a recoil of 400G, resulting in stresses mainly in the holes of the fixture represented by a color scale. The maximum stress is recorded to 135,4MPa.

6.3 Tests

For the recoil tests, only the first shock of each test will be shown. The rest can be found in the appendix, see figures 43-52. The signals received during this test were the strain of one bolt in each direction, one normal and one perpendicular to the recoil direction, and the accelerations from the middle weight of the fixture. These can be seen in figures 29-32.

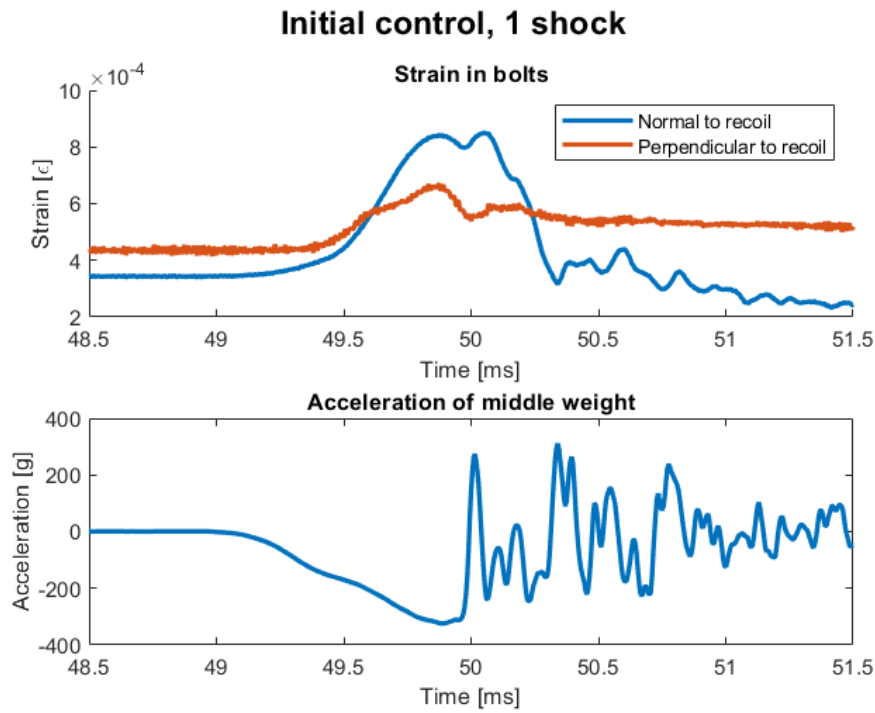


Figure 29: Strain measured in the bolts of each direction during the initial control test and the accelerations from the middle weight of the fixture.

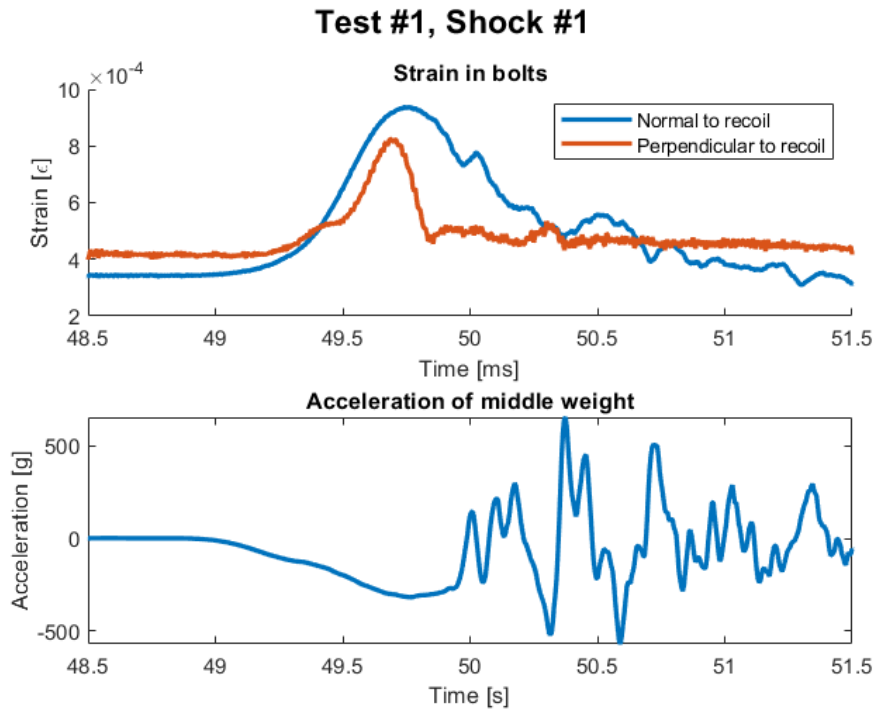


Figure 30: Strain measured in the bolts of each direction during the first shock of the first test and the accelerations from the middle weight of the fixture.

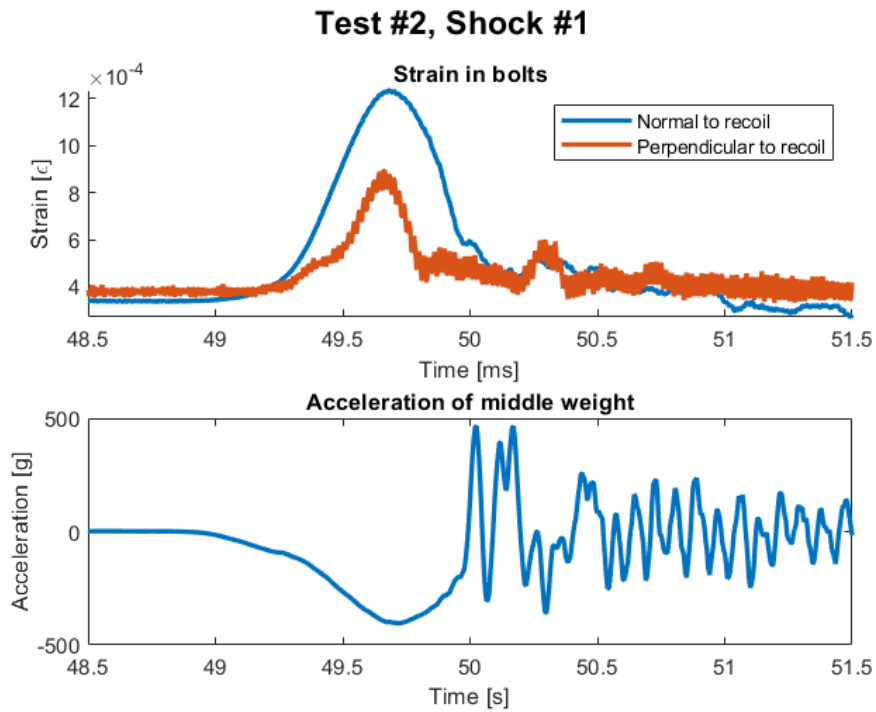


Figure 31: Strain measured in the bolts of each direction during the first shock of the second test and the accelerations from the middle weight of the fixture.

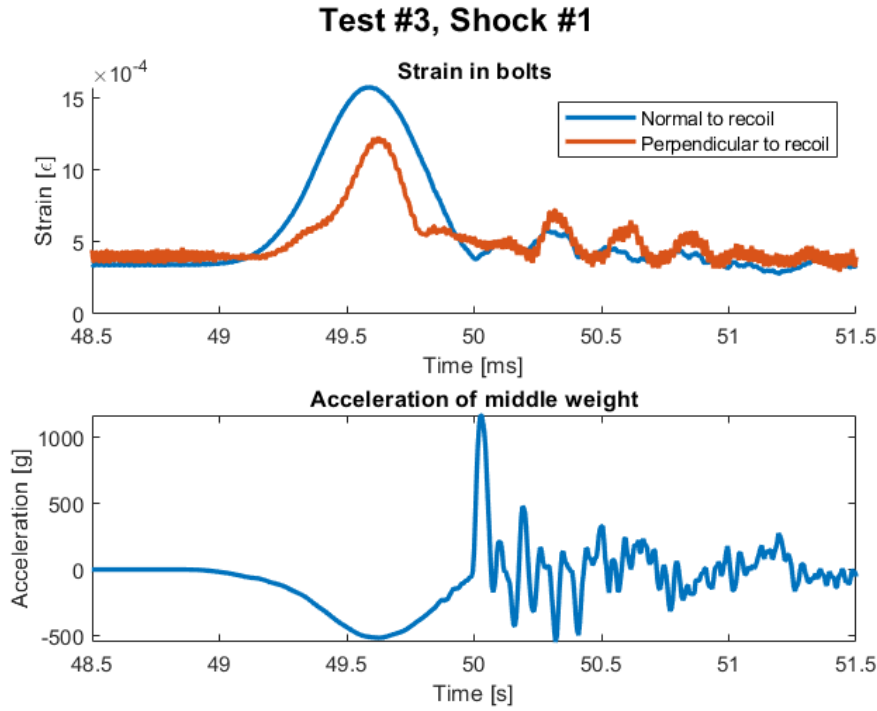


Figure 32: Strain measured in the bolts of each direction during the first shock of the third test and the accelerations from the middle weight of the fixture.

The strain can be translated to force with the use of equation (13) and the acceleration can be translated with the use of equation (14). This way, the force from the acceleration of the middle weight and the force from the strain of the bolt holding the same weight can be compared. This can be seen in table 7. In table 8 the maximum value of the acceleration curves from the shock machine are compared to the maximum values of the acceleration of the weight.

Test / Shock	Max force from strain [N]	Max force from acc. [N]	Difference [N]
Initial / 1	6224	7116	-892
1 / 1	6862	6961	-99
1 / 2	6771	6611	160
1 / 3	6788	6457	337
2 / 1	9046	8879	167
2 / 2	9543	9050	493
2 / 3	9740	9164	576
3 / 1	11523	11294	229
3 / 2	13539	13653	-114
3 / 3	14740	15360	-620

Table 7: The maximum forces translated from strain in the strain gauges in the bolts and from the accelerometer on the middle weight of the fixture.

Test / Shock	Max acc. of weight	Max acc. from machine	Difference
Initial / 1	324,06	460,28	136,23
1 / 1	317,02	415,36	98,341
1 / 2	307,02	398,23	91,212
1 / 3	294,06	404,60	110,55
2 / 1	404,37	475,50	71,13
2 / 2	412,15	491,35	79,2
2 / 3	417,33	485,44	68,105
3 / 1	514,37	558,25	43,883
3 / 2	621,77	564,11	-57,668
4 / 3	699,55	552,39	-147,16

Table 8: The maximum accelerations measured from the accelerometers on the middle weight of the fixture and on the "table" of the shock machine Elstar.

During the tests, there was a noticeable difference between the start- and end-points of the shocks. These can be seen in figure 33. They have been assigned the same time scale for easy comparison and the first shock is zeroed and then the tightening strain is applied.

Comparison of the three shocks in...

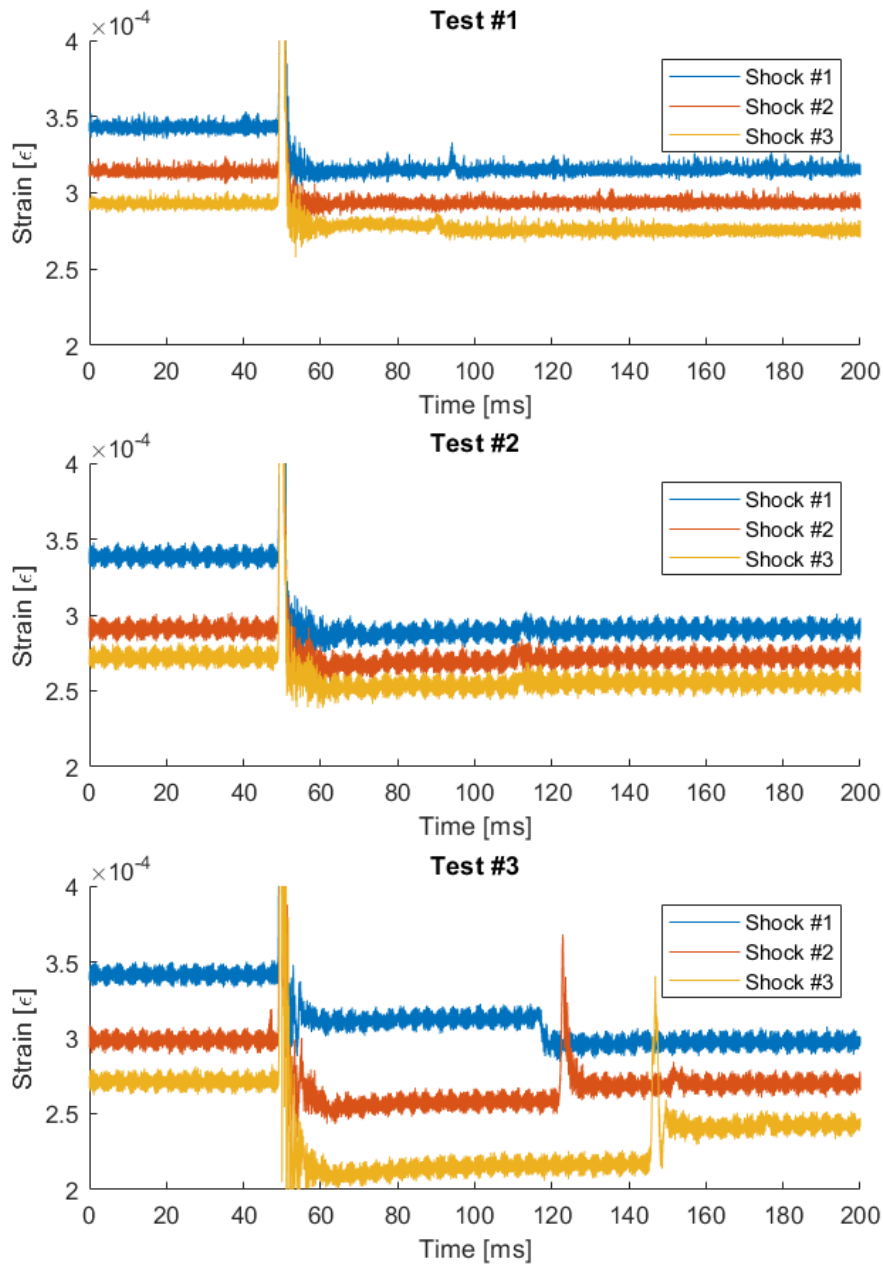


Figure 33: The strain compared of the three shocks in succession to each other for each test. All shocks have been assigned the same time scale for easy comparison.

6.4 FEM verification of recoil test

The simulations replicate the experiments as close as possible and the bolts were modeled according to three different methods: coupled-, hybrid- and solid bolt. Results from simulations with major changes can be found in figures 34 to 40. The initial simulation is from before the test and is used as a base. It is a coupled bolt with a

translator connector without behaviors and a hold condition after the tightening.

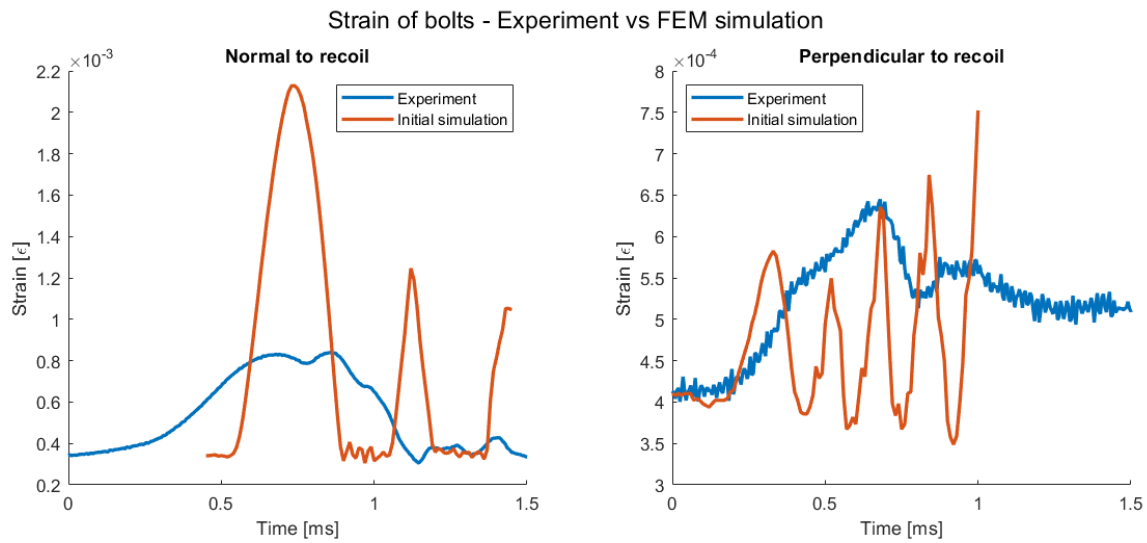


Figure 34: Initial simulation is used as a base consisting of coupled bolt with a translator connector without behaviors and a hold condition after the tightening (orange). The simulation is compared to the experimental data (blue).

The second result takes the initial simulation and adds elasticity and a reference length on the translator. With the reference length, the hold condition is removed since the shorter length is the new tightening condition.

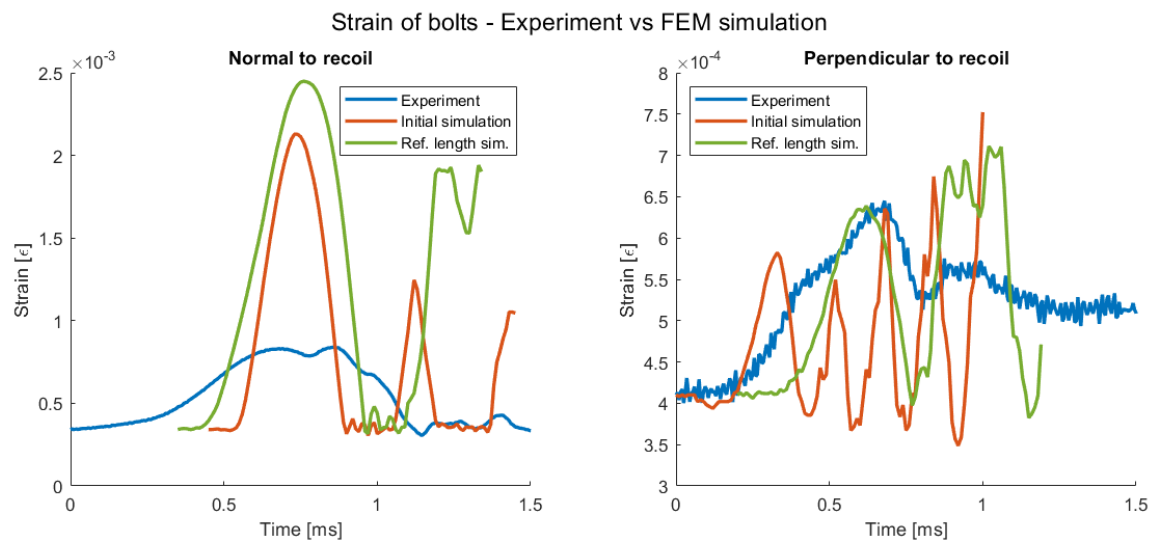


Figure 35: Initial simulation is used as a base consisting of coupled bolt with a translator connector without behaviors and a hold condition after the tightening (orange). Ref. length sim. is the same coupled bolt but with elasticity, a reference length and the hold condition is removed (green). The simulations are compared to the experimental data (blue).

Changing the translator connector to an axial connector with the same behaviors gives the third result.

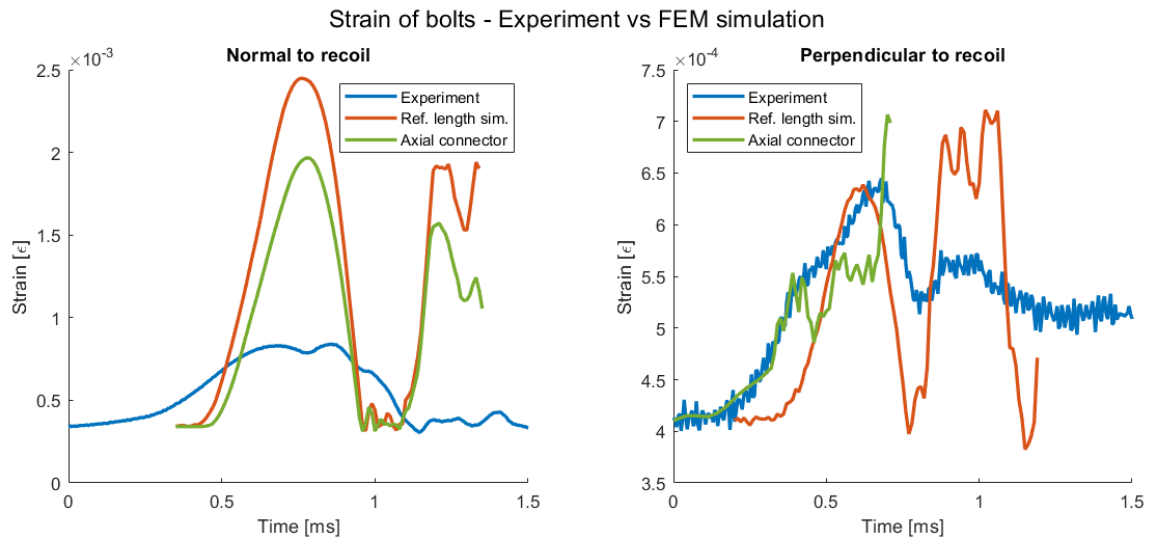


Figure 36: Ref. length sim. is a coupled bolt but with elasticity, a reference length and the hold condition is removed (orange). The same simulation but with an axial connector instead of a translator (green). The simulations are compared to the experimental data (blue).

Since the last result was the best that could be reached when only looking at connectors, behaviors and conditions, more detailed settings were altered such as mass scaling and damping. Changing the mass scaling target time increment from 1E-08 to 1E-09 gives the result below. Adding a damping of 1 gave the exact numerical result.

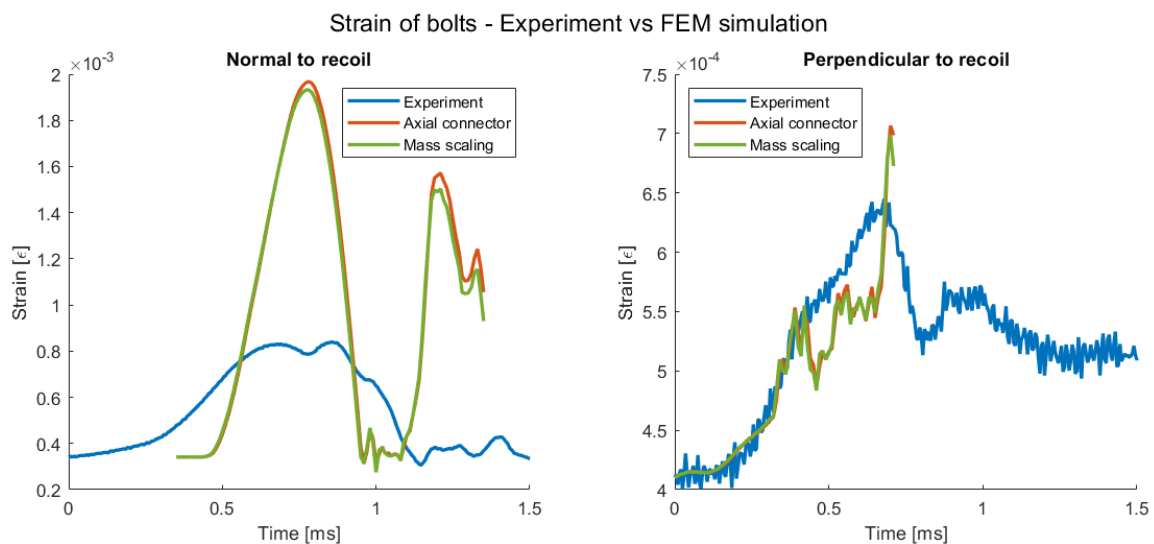


Figure 37: Axial connector is a coupled bolt with elasticity and a reference length (orange). The same simulation but with a change in mass scaling (green). The simulations are compared to the experimental data (blue).

The aim was to replicate the test, but there was a mistake in how the recoil curve was modeled. The experiment had a half sine curve with a half time period of 0.8ms, while the half time period in the simulation was 0.5ms. After changing the curve in the simulation, it gave the following result below.

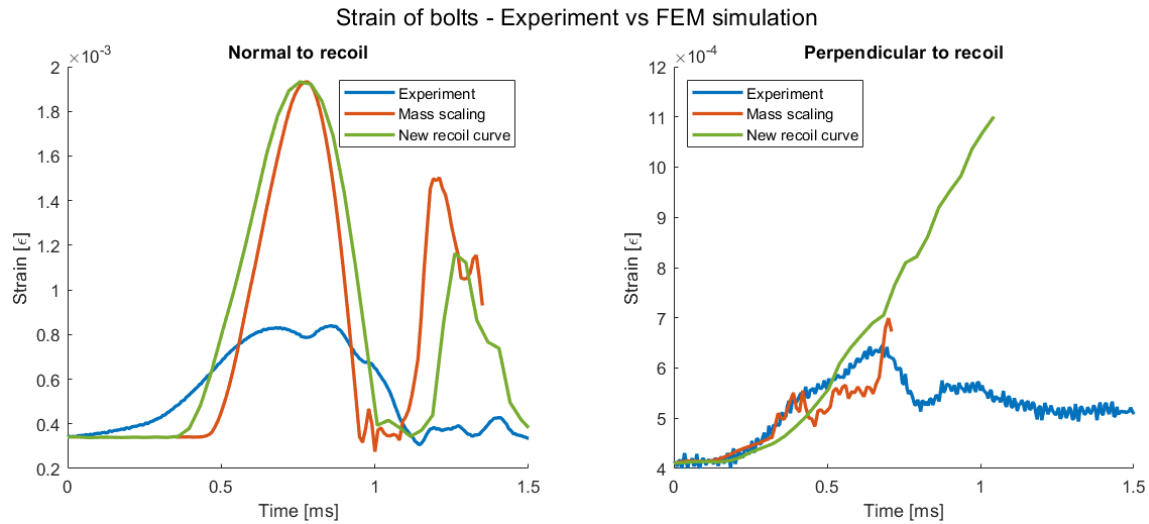


Figure 38: Mass scaling is a coupled bolt with an axial connector with elasticity and a reference length (orange). The same simulation but the mass scaling is changed back and the recoil is changed to match the experiment's time period of 0.8ms (green). The simulations are compared to the experimental data (blue).

There was a plateau in what could be achieved with the coupled bolt simulations. The next simulation is of the hybrid bolt with an axial connector with the same behaviors as before.

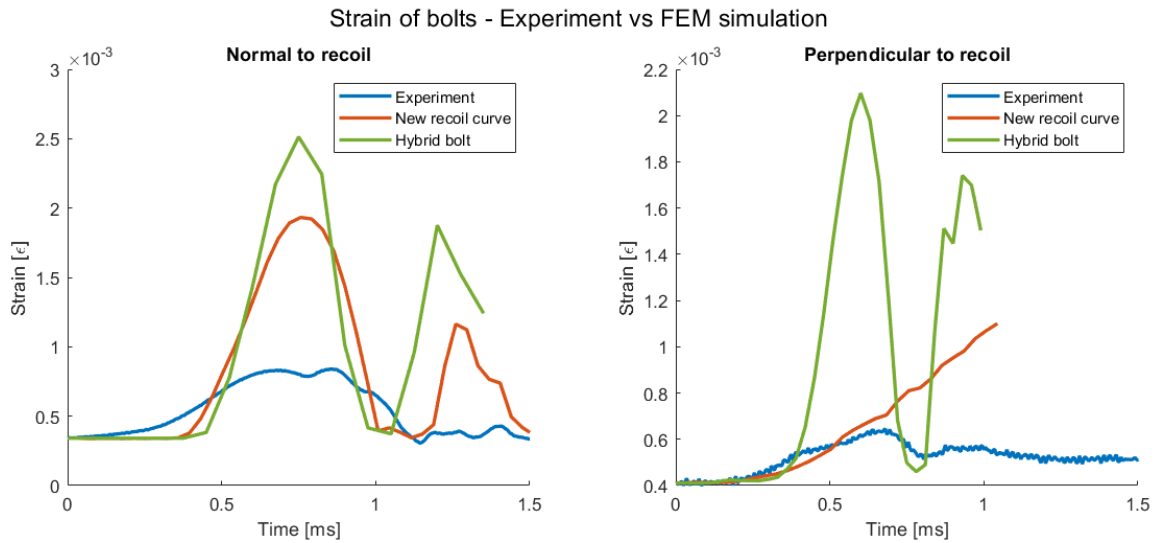


Figure 39: New recoil curve is a coupled bolt with an axial connector with elasticity, a reference length and a recoil curve that matches the experimental time period (orange). The same simulation but the bolt is changed from coupled to hybrid with elasticity and a reference length (green). The simulations are compared to the experimental data (blue).

As the result worsened, there was no dwelling on the hybrid bolt and quickly moved on to the last simulation: the solid bolt.

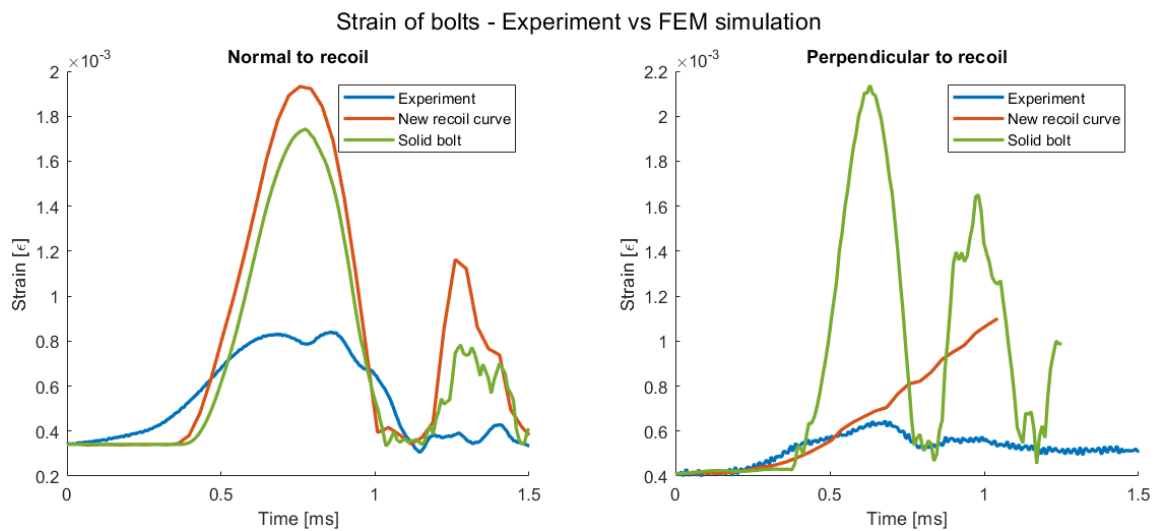


Figure 40: The solid bolt has the behaviors that come with the material assignment, in this case steel (orange). New recoil curve is a coupled bolt with an axial connector with elasticity, a reference length and a recoil curve that matches the experimental time period (green). The simulations are compared to the experimental data (blue).

7 Discussion

This chapter will provide more in depth interpretation of the results and the possible errors that entails, to then see if they agree with the goals of this project. First, the test methodology will be evaluated which then will lead into the methodology of the FEM-simulations and the results that were generated. Second, existing errors and their improvements will be presented. Lastly, suggestions for future work.

7.1 Test methodology

The test methodology consisted of 3D modeling a fixture, initial FEM-simulations and the experiments. The design was dependent on the existing machines and their fasteners, and how the in-house manufacturing is able to create models. The first iteration of designs were modeled as one combined piece, but the workshop declined these models due to the complex milling it would entail. Using 5000N as maximum load for the quasi-static test gave adequate results, but I do believe that the designs could be improved. For the bolt model of the quasi-static test, the disk in top slot of the fixture is not reliable as it created a hole in the house where the pinholes are located. As seen in figure 23, there is a lot of stress in that area. The highest stress in that model, which can be located on the bottom plate, can be disregarded since it is held down by boundary conditions instead of bolts. This creates a sharp unrealistic edge, where the elements connected to this edge are deformed more than what is realistic. Therefore, the green areas are of interest. These can be found around the pin holes, top corners of the house and the bolt hole in the house and the bottom plate. In the end, the model worked as intended. Both models of the quasi-static test gave results that matched the theoretical values of strain very well. For the actual test, the only other way this could have been done would have been through compression or bending, but for the purpose of applying normal strain to a bolt during recoil, the tension test was a reliable method to see how the strain gauges would behave.

Similarly for the fixture for the recoil test, the design could not be too complex for the workshop to create and it also had a weight limit for the machine. The model did not exceed these conditions and showed the results in figure 28. The simulation did not show any high stresses except in the bolt holes, which means that the fixture was stable and that the bolts would be the main focus. With the use of a bolt with a smaller radius, the fixture and the weights could have been lighter, but since the bolt needed a 2mm wide hole drilled into it, a smaller bolt would not have been suitable. The test was deemed as successful since the force measured in table 7 only have a slight difference. As the accelerometer was placed on the weight and is compared to the bolt that holds the weight, a difference is expected due to the energy dissipation throughout the fixture.

7.2 FEM-verifications of bolts during recoil

The verification simulations of the recoil test did not satisfy the goal of this project, but it is a step forward and will contribute to future simulations. The initial simulation

in figure 34 was based on past simulations done at Aimpoint to get a baseline for how Abaqus works and to get an idea for how they model bolts. All simulations resulted in a strain normal to the recoil that was around two to three times larger than the strain from the experiment. The simulations of the bolt perpendicular to the recoil did not emulate the experiment until the later simulations. However, the peaks of the initial simulation were proportional to the test of the bolt normal to the recoil. This simulation had a translator and a hold condition on the bolts which was applied after tightening the bolts. This resulted in a stiff bolt that did not allow for any damping. The next simulation, "Ref. length sim.", removed the hold condition and had a reference length set to replace the tightening load. Unfortunately, this gave a higher curve but it allowed for some reaction time to the recoil, which can be seen at the base of the curve. The initial simulation has a reaction time of exactly 0,5ms, while the next simulation has a reaction time of 0,8ms. The experiment has a reaction time of 1,2ms. The strain in the bolt perpendicular to the recoil is still increasing with each shock, matches the experiment better than the initial simulation.

This is then used as comparison with the third simulation, "Axial connector". Here, the same setting are used but with an axial connector instead of a translator. As mentioned in the glossary, the nodes of the axial connector are not locked to each other as they are for the translator. This gives a less stiff bolt which can be seen in figure 36 as the curves are quite similar, but the axial bolt is dampened. This did however not improve the result of the bolt perpendicular to the recoil, but these settings were chosen as the most optimal and were then to be fine-tuned with mass scaling and damping. Figure 37 contains the result, "Mass scaling" of changing the mass scaling target time from 1E-08 to 1E-09. This did not have a significant impact on the result and only cost more in computational time. The damping result is not included since it resulted in the exact same result as the mass scaling and there is no explanation to why. The last change to the coupled bolt was to redefine the recoil curve and was named "New recoil curve". It was discovered that the recoil of Elstar was 0,8ms instead of 0,5ms, but it was still a half sine curve, therefore only the half period time was changed.

The last two simulations done were of the hybrid bolt and the solid bolt. Unfortunately, the hybrid bolt did not give an improvement to the bolt normal to the recoil. However, the bolt perpendicular to the recoil was improved in terms of how it reacts to the shock. The strain did not increase after the initial shock and was instead dampened. The peaks are about three times higher, but are proportional to the peaks of the experiment. Similarly, this can be seen for the solid bolt, but the simulation of the bolt normal to the recoil had the greatest improvement. The peak is just above two time higher than in the experiment, but has a reaction time of 0,6ms.

7.3 Sources of error

The fixture for the recoil test was sent for manufacturing and had a long lead time. During this time, all the preparations of fixing the bolts and soldering all cables and connector. However, when soldering the gauges to the cables a sudden realization hit me. The cords of the strain gauges are in the way for the Allen key that was going

to be used to tighten the bolts. Since the design already was sent for manufacturing, it could not be changed. To tackle this problem, a canal was dremeled into the bolt where the cords could be glued into. More bolt had to be prepared in case they broke during mounting of the fixture, which did indeed happen. This could have been avoided by using a bolt with a hex-head and an open wrench, in hindsight, but I had to make due.

As seen in figure 33, each shock resulted in a lower strain in the bolt than what it started with. The end of the first shock is the start of the second shock and so on. In the second test, there is a visible disturbance around 110ms, which is interpreted as a second shock which is when the weight bounces after the recoil. These disturbances are then magnified in the third test which increases with each shock. This can be interpreted as the bolt no longer being tightened and the weight is loose, which means that the bolt is either plastically deformed or the bolt has come loose due to the shock and vibrations. I believe it is the former since the bolt was calculated to withstand around 400G and Elstar is not precise. In table 8, it can be seen that the initial test resulted in an acceleration of 460G even though the height of the table was the same as for test 1. After the first test was done, the table height was deliberately increased even though knowing that the bolt might not hold. This was due to the machine showing one value, while the accelerometer on the middle weight showed another. It wasn't until the second test that the weight reached 400G, but the third test was done to test the limits of the bolt. It can be seen in the same table that the acceleration of the weight increases with each shock in the third test, which could show that the weight was hanging more freely before the shock and deformed the bolt more with each shock.

One mistake with the simulations was that it was not noticed until later that the half sine defined in the simulations did not match the curve derived in the experiment. This should have been taken care of from the beginning, but it was a misinterpretation of the data provided by Elstar. There exists other user errors in the simulations due to the fact that Abaqus was a new program to me and was not intuitive to learn. Use was made of the handbook and colleagues, but there were probably still some misunderstandings of what the settings mean, how they should be used and how to interpret their results.

7.4 Future work

There is more work to be done before the second goal of this project can be fulfilled. Using the simulations to develop test will give a substantial margin of error so that the designs will not be sufficiently tested. The future work should consist of continued work on the bolt models and their different settings and features. There are more than just three bolt models, but I do not believe that any other variation would contribute to a more drastic change. But just for interest sake, more models can be looked into.

The perpendicular bolt analyzed with the shearing strain was the weak point of this project. The simulations were unreliable as the strain and energy increased with each bounce after the recoil. There was no understanding of why and was pushed to the side, while the main focus was on the bolt normal to the recoil. Perhaps, these

different cases should not have been tested together. It was done this way due to time and manufacturing efficiency. If there is a need to separate these cases, the bolt should be positioned so that the weight rests on the fixture and the recoil is applied from the side. Therefore, the bolt will have a more rested position as it does not have to hold up the weight before the recoil and it will better simulate how bolts used for Aimpoint's fasteners work.

8 Conclusion

To conclude this report, one out of the two goals of this project were successful. A test methodology for measuring strain in bolts during recoil was developed and functional. As for now, using FEM-simulations to verify if models of bolts are suited for recoil exposure is not reliable. Using the simulations to develop test will give a substantial margin of error that the designs will not be sufficiently tested. However, there is more to study in this area and this project will contribute to further investigations. Based on this project, the model to be used if needed should be the solid bolt, but the investigation should not exclude the hybrid and coupled bolt since they could be used to make the computational time shorter and the simulations more efficient.

References

- [1] Aimpoint AB, “Our History,” [Online]. Available: <https://www.aimpoint.com/about-us/our-history/>.
- [2] R. K. Rajput, *Engineering Thermodynamics*. LAXMI PUBLICATIONS (P) LTD, 2007, ISBN: 978-0-7637-8272-6.
- [3] K. Behan, E. Guzas, J. Milburn, and S. Moss, “Finite element modeling of k-monel bolts under static loading and dynamic shock loading,” *Shock and Vibration*, vol. 20, 2012. DOI: <https://doi.org/10.3233/SAV-130769>.
- [4] N. S. Ottosen and H. Petersson, *Introduction to the Finite Element Method*. Prentice Hall Europe, 1992, ISBN: 0-13-473877-2.
- [5] J. Kim, J.-C. Yoon, and B.-S. Kang, “Finite Element Analysis and Modeling of Structure with Bolted Joints,” *Applied Mathematical Modelling*, vol. 31, no. 5, pp. 895–911, 2007. DOI: <https://doi.org/10.1016/j.apm.2006.03.020>.
- [6] A. Korolija, “FE-modeling of Bolted Joints in Structures,” 2012.
- [7] Fastenal Engineering & Design Support, “Bolted Joint Design,” vol. Rev 3-4-2009, 2009.
- [8] J. Gattmah, S. K. Shihab, M. T. Mohamed, and A. L. Abbas, “Effects of Increasing Mass Scaling in 3D Explicit Finite Element Analysis on the Wire Drawing Process,” *IOP Conference Series: Materials Science and Engineering*, vol. 1076, 2021. DOI: <https://doi.org/10.1088/1757-899X/1076/1/012072>.
- [9] S. Timoshenko, *Strength of Materials, Part 1: Elementary Theory and Problems*, 2nd ed. D. Van Nostrand Company, Inc, 1940.
- [10] *Getting started with abaqus*, ABAQUS Inc., 2006, ch. 5.2 Plasticity in ductile metals. [Online]. Available: <https://classes.engineering.wustl.edu/2009/spring/mase5513/abaqus/docs/v6.5/books/gsx/default.htm?startat=ch05s02.html>.
- [11] Avdelningen för Hållfasthetslära, *Hållfasthetslära för F, Utdrag ur: Instruktion till Hållfasthetslära, Enaxliga tillstånd, Ljung et al. Instruktion till Hållfasthetslära, Allmänna tillstånd, Ottosen et al.* Lunds Universitet.
- [12] HBM, “How does an electrical strain gauge work?,” [Online]. Available: <https://www.hbm.com/en/7328/how-does-an-electrical-strain-gauge-work/>.
- [13] HBM, “The wheatstone bridge circuit explained,” [Online]. Available: <https://www.hbm.com/en/7163/wheatstone-bridge-circuit/>.
- [14] J. Fraden, *Handbook of Modern Sensors - Physics, Design, and Applications*, 5th ed. Springer International Publishing, 2016, ISBN: 978-3-319-19302-1. DOI: <https://doi.org/10.1007/978-3-319-19303-8>.
- [15] R. Lee, *ABAQUS for Engineers, a Practical Tutorial Book*. BW Publications, 2018, ISBN: 9791163471264.

- [16] K.-J. Bathe, *Finite Element Procedures*. Prentice-Hall Inc., 1996, ISBN: 0-13-301458-4.
- [17] M. Ålenius, “Finite Element Modelling of Composite Bridge Stability,” 2003.
- [18] P. Langer, K. Sepahvand, C. Guist, and S. Marburg, “Finite Element Modeling for Structural Dynamic Analysis of Bolted Joints Under Uncertainty,” *Procedia Engineering*, vol. 199, pp. 954–959, 2017. DOI: <https://doi.org/10.1016/j.proeng.2017.09.199>.
- [19] N. E. A. Subki, H. Mansor, Y. S. Hamid, and G. Parke, “Finite Element Dynamic Analysis of Double-Span Steel Beam Under an Instantaneous Loss of Support,” *Proceedings of the 5th International Conference on Sustainable Civil Engineering Structures and Construction Materials. SCESCM 2020. Lecture Notes in Civil Engineering*, vol. 215, pp. 593–610, 2022. DOI: https://doi.org/10.1007/978-981-16-7924-7_39.
- [20] *Abaqus analysis user’s manual*, ABAQUS Inc., 2006, ch. 25.1.5 Connection-type library. [Online]. Available: <https://classes.engineering.wustl.edu/2009/spring/mase5513/abaqus/docs/v6.6/books/usb/default.htm?startat=pt06ch25s01aus92.html>.
- [21] MatWeb, “Aluminum 6082-T6,” [Online]. Available: <https://www.matweb.com/search/datasheet.aspx?matguid=fad29be6e64d4e95a241690f1f6e1eb7>.
- [22] MatWeb, “Aluminum, Al,” [Online]. Available: <https://www.matweb.com/search/datasheet.aspx?bassnum=AMEAL00>.
- [23] MatWeb, “AISI 4140 Steel,” [Online]. Available: <https://www.matweb.com/search/DataSheet.aspx?MatGUID=1897ec2242d14abba04ef1de7e7be01d&ckck=1>.
- [24] HBM, “LY Linear Strain Gauges with 1 Measuring Grid,” [Online]. Available: https://www.hbm.com/en/4561/ly-linear-strain-gauges-with-1-measurement-grid/?product_type_no=LY%20Linear%20Strain%20Gauges%20with%201%20Measuring%20Grid.
- [25] HBM, “LB11 & TB21: Strain gauges for measurements in screws and bolts,” [Online]. Available: https://www.hbm.com/en/7452/cylindric-strain-gauges-for-measurements-in-bolts/?product_type_no=LB11/TB21%20Strain%20Gauges%20for%20Measuring%20in%20Screws%20&%20Bolts.
- [26] Dewesoft, “Strain Measurement Using Strain Gage Sensors,” [Online]. Available: <https://training.dewesoft.com/article/course/strain-measurement-using-strain-gage-sensors#wheatstone-bridge>.

9 Appendix

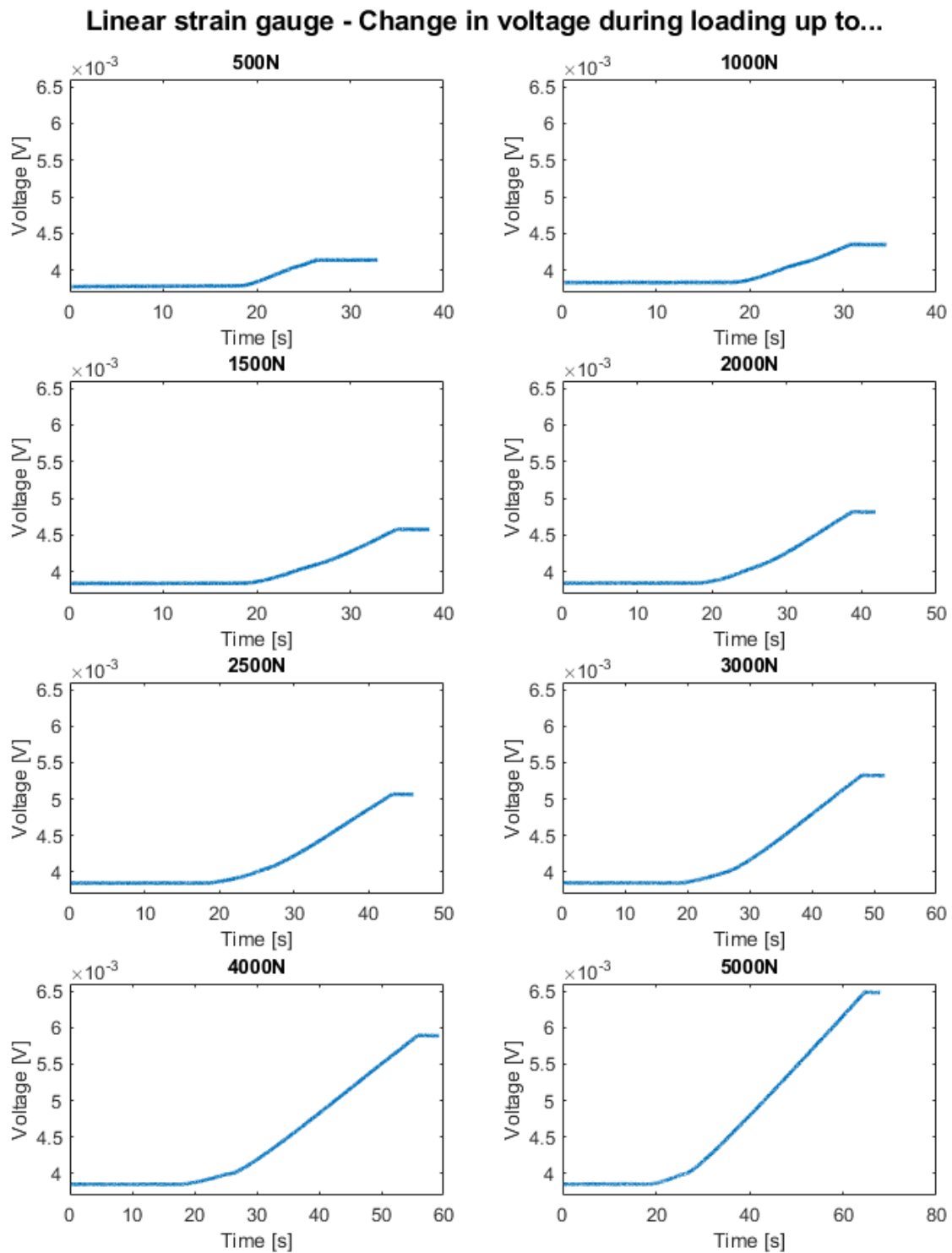


Figure 41: Voltage measurement during a quasi-static loading of 500N-5000N of a linear strain gauge.

Cylindrical strain gauge - Change in voltage during loading up to...

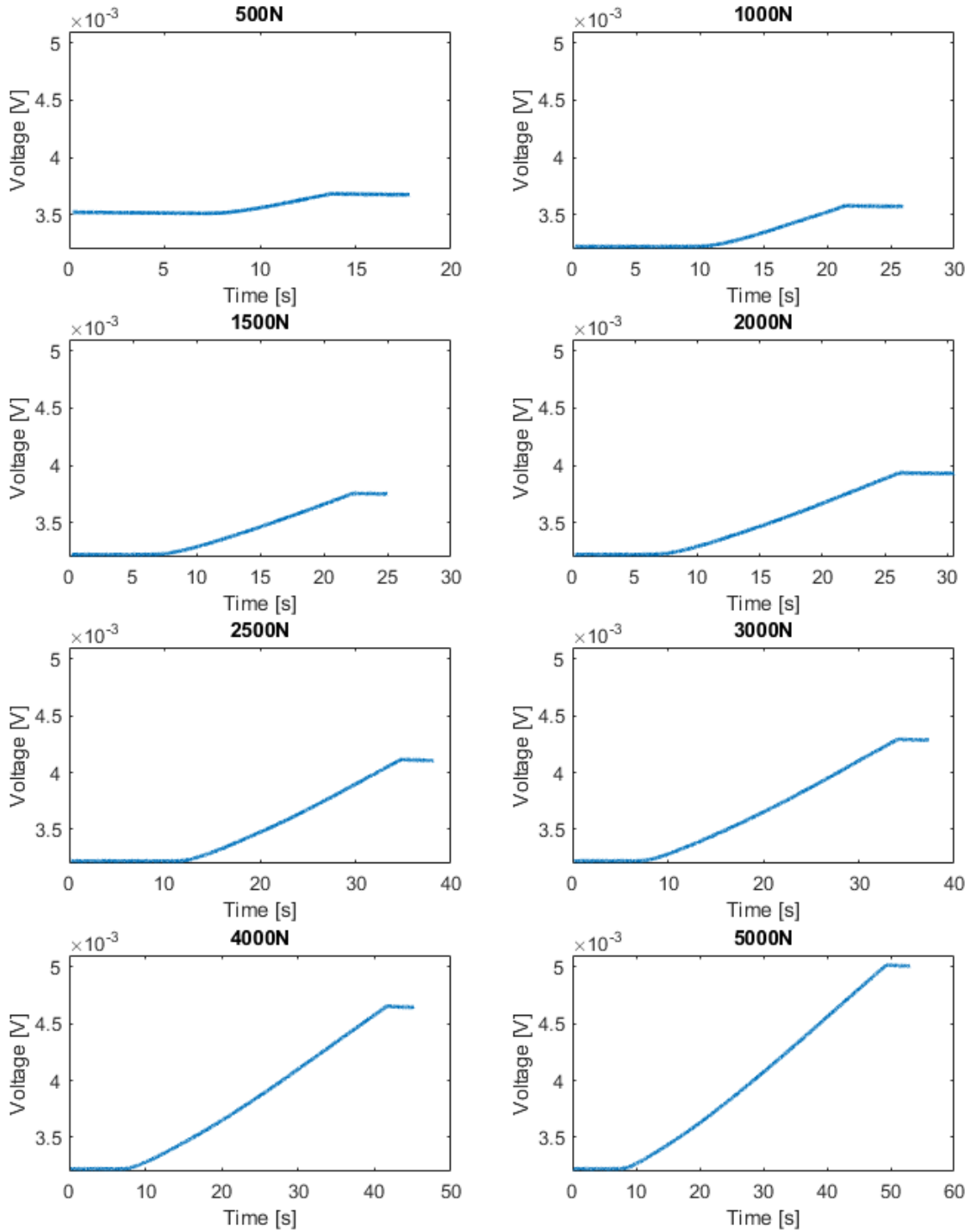


Figure 42: Voltage measurement during a quasi-static loading of 500N-5000N of a cylindrical strain gauge.

Load [N]	Max V_0 [V, E-3]	Min V_0 [V, E-3]	ΔV_0 [V, E-3]
500	4,141	3,778	0,363
1000	4,353	3,834	0,519
1500	4,580	3,842	0,739
2000	4,818	3,845	0,973
2500	5,068	3,847	1,221
3000	5,327	3,849	1,478
4000	5,893	3,851	2,042
5000	6,485	3,854	2,631

Table 9: Difference in voltage of the linear strain gauge during different loading tests.

Load [N]	ϵ , measured [E-4]	ϵ , calculated [E-4]	$\Delta\epsilon$ [E-4]
500	1,418	1,006	0,412
1000	2,026	2,012	0,013
1500	2,883	3,018	-0,136
2000	3,796	4,024	-0,228
2500	4,766	5,030	-0,264
3000	5,766	6,036	-0,270
4000	7,969	8,048	-0,079
5000	10,268	10,060	0,208

Table 10: Difference in strain of the linear strain gauge during different loading tests while measuring output voltage.

Load [N]	Max V_0 [V, E-3]	Min V_0 [V, E-3]	ΔV_0 [V, E-3]
500	3,683	3,511	0,172
1000	3,579	3,221	0,358
1500	3,757	3,220	0,537
2000	3,936	3,222	0,714
2500	4,114	3,221	0,893
3000	4,293	3,222	1,071
4000	4,652	3,221	1,431
5000	5,017	3,221	1,796

Table 11: Difference in voltage of the cylindrical strain gauge during different loading tests.

Load [N]	ϵ , measured [E-4]	ϵ , calculated [E-4]	$\Delta\epsilon$ [E-4]
500	0,672	0,683	-0,011
1000	1,398	1,366	0,032
1500	2,095	2,049	0,046
2000	2,788	2,732	0,056
2500	3,485	3,415	0,070
3000	4,181	4,098	0,083
4000	5,583	5,464	0,118
5000	7,008	6,831	0,178

Table 12: Difference in strain of the cylindrical strain gauge during different loading tests while measuring output voltage.

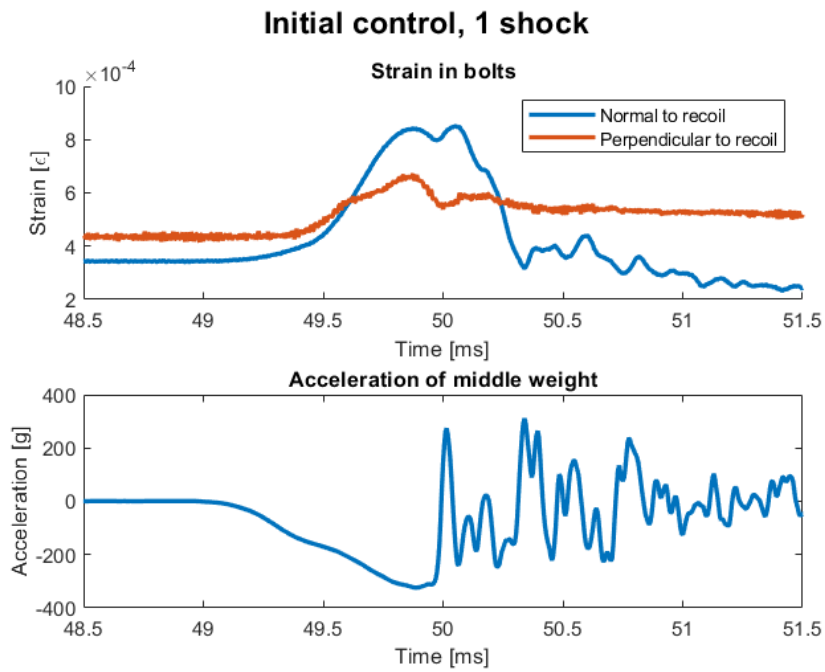


Figure 43: Strain measured in the bolts of each direction during the initial control test and the accelerations from the middle weight of the fixture.

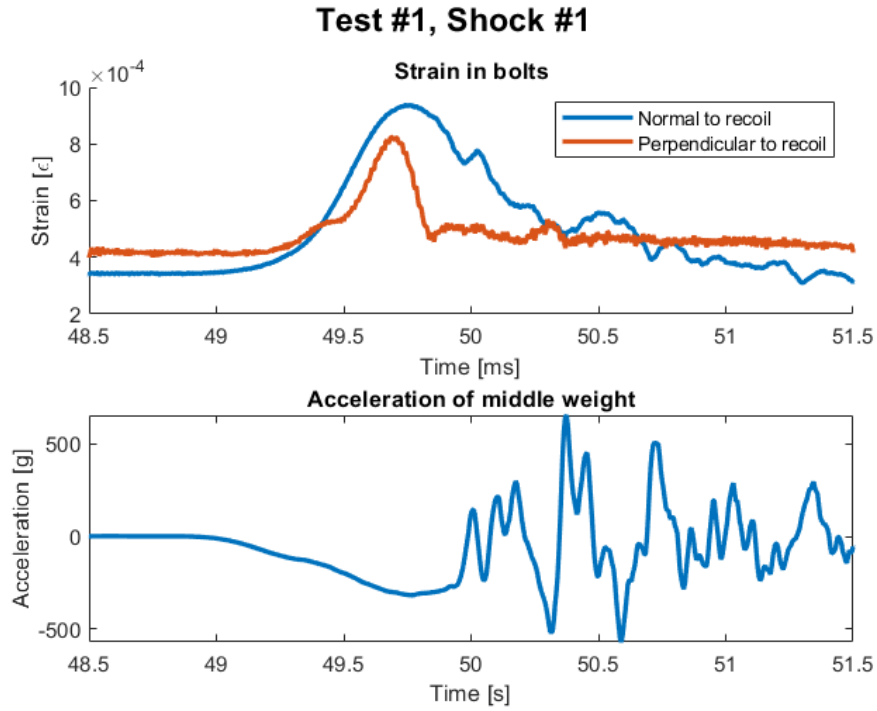


Figure 44: Strain measured in the bolts of each direction during the first shock of the first test and the accelerations from the middle weight of the fixture.

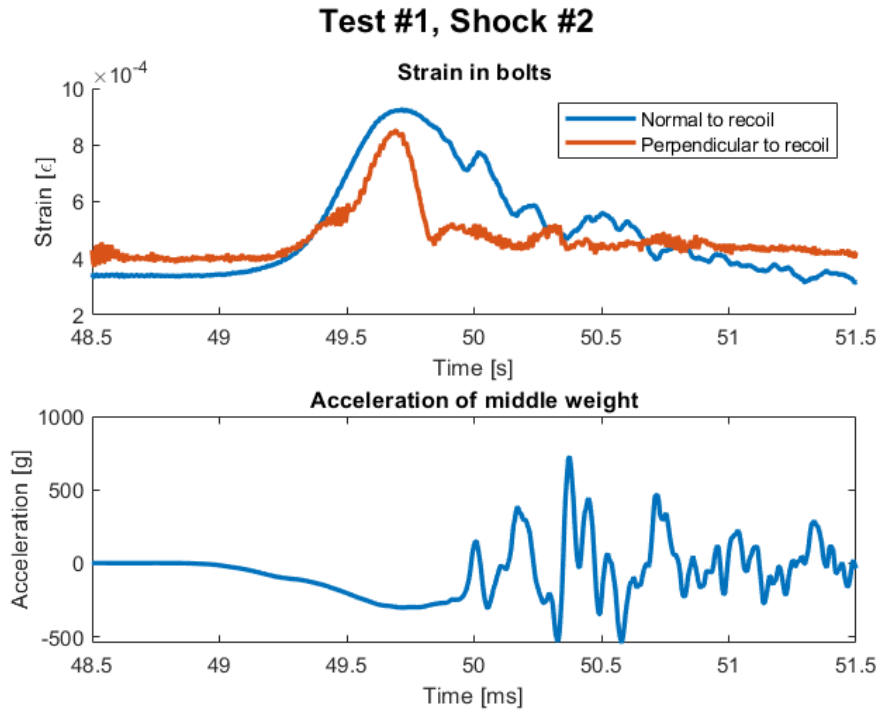


Figure 45: Strain measured in the bolts of each direction during the second shock of the first test and the accelerations from the middle weight of the fixture.

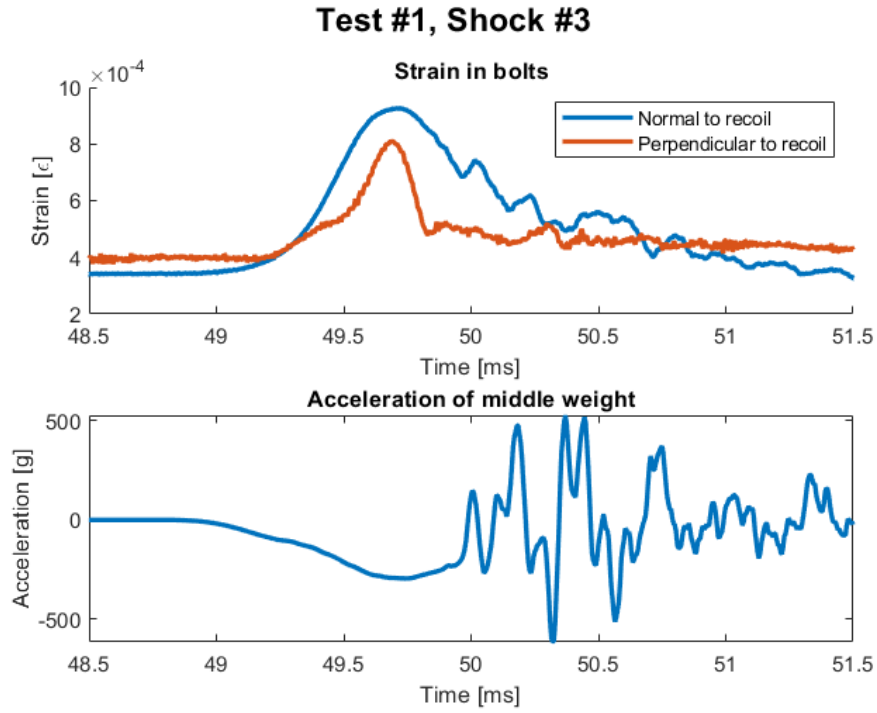


Figure 46: Strain measured in the bolts of each direction during the third shock of the first test and the accelerations from the middle weight of the fixture.

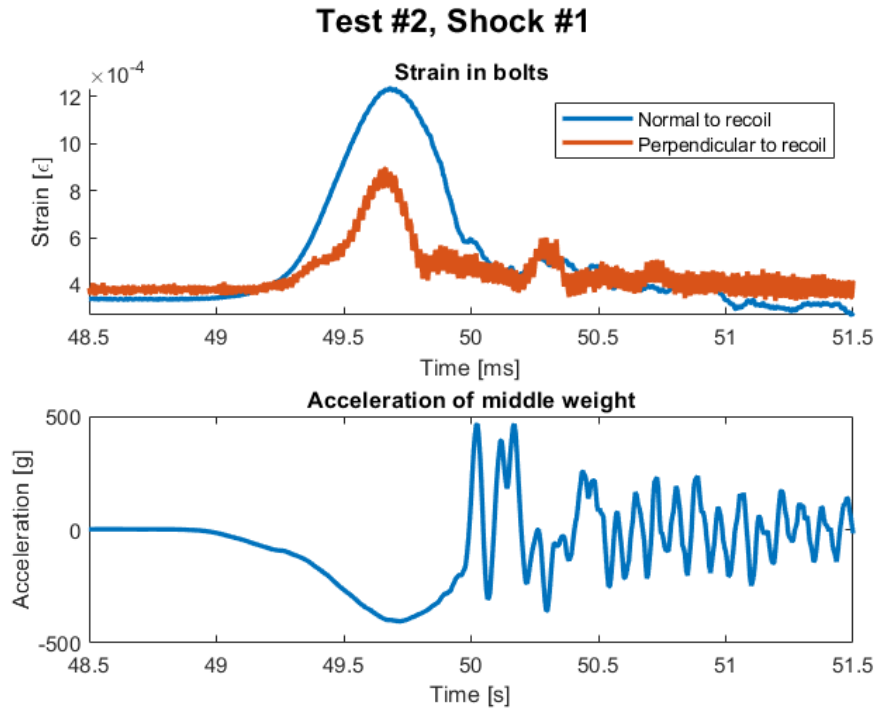


Figure 47: Strain measured in the bolts of each direction during the first shock of the second test and the accelerations from the middle weight of the fixture.

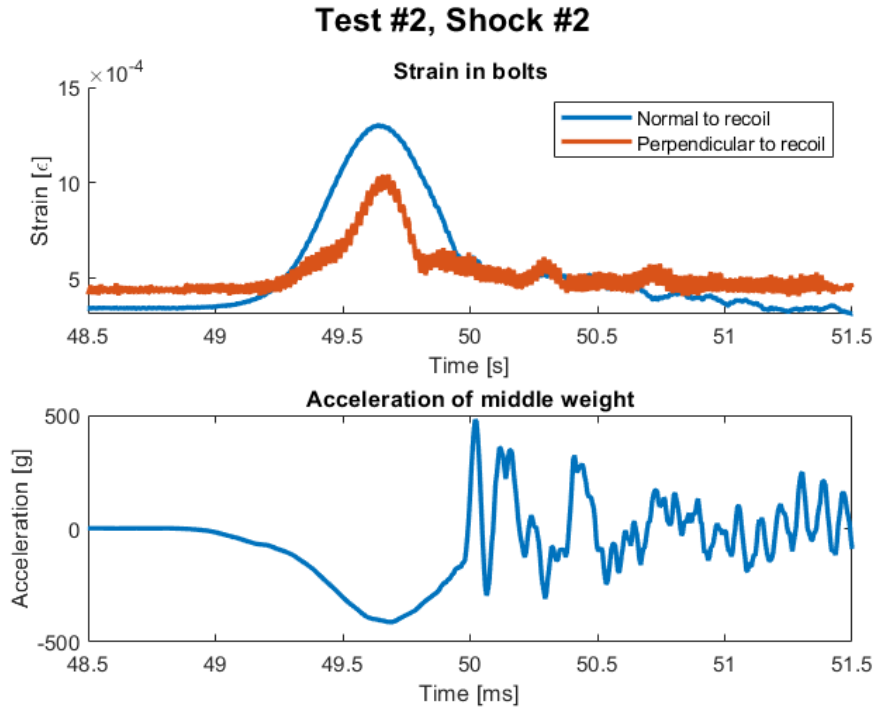


Figure 48: Strain measured in the bolts of each direction during the second shock of the second test and the accelerations from the middle weight of the fixture.

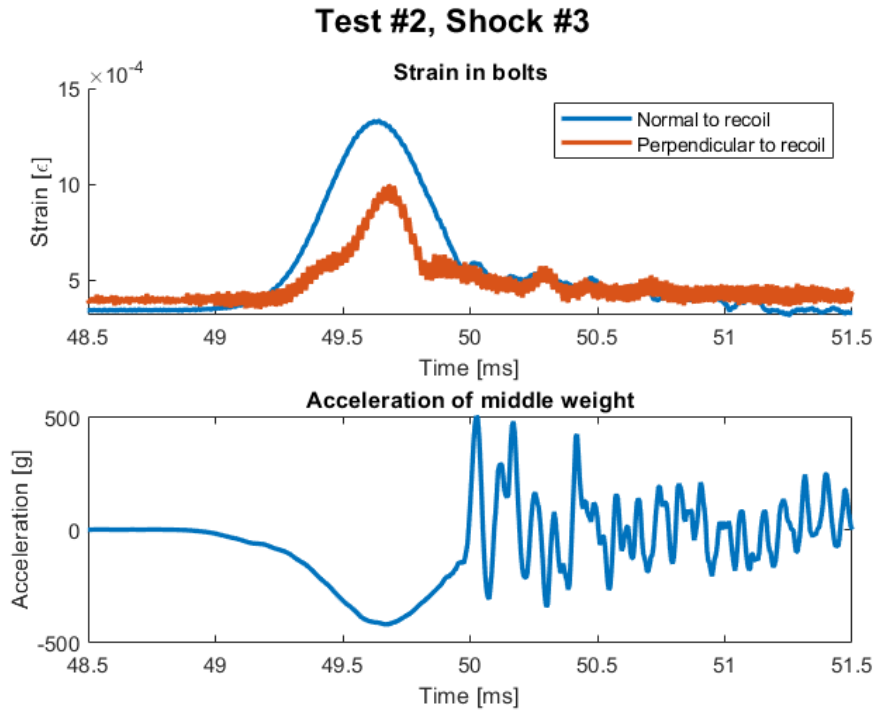


Figure 49: Strain measured in the bolts of each direction during the third shock of the second test and the accelerations from the middle weight of the fixture.

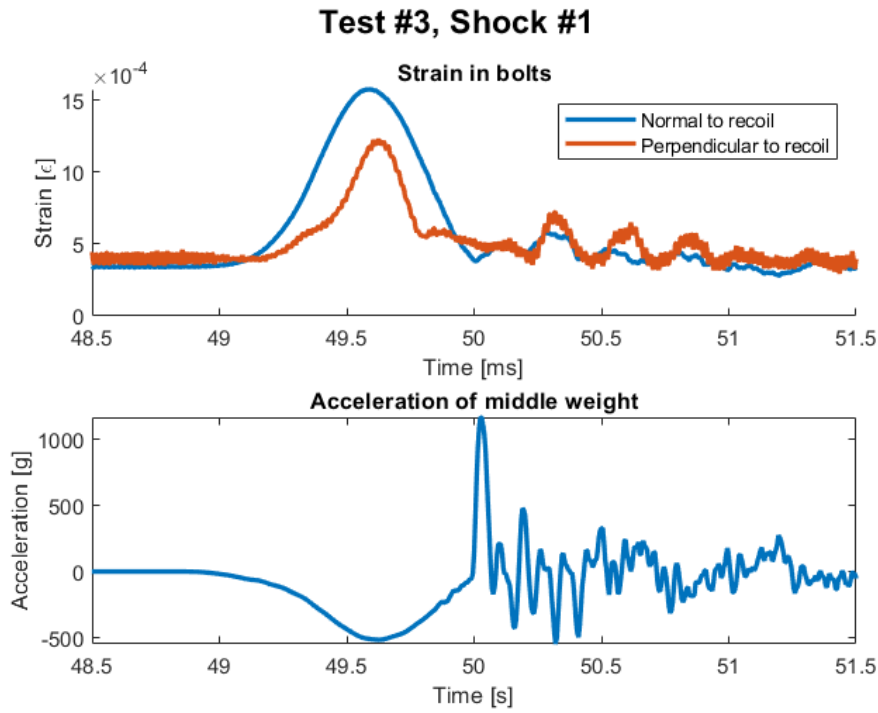


Figure 50: Strain measured in the bolts of each direction during the first shock of the third test and the accelerations from the middle weight of the fixture.

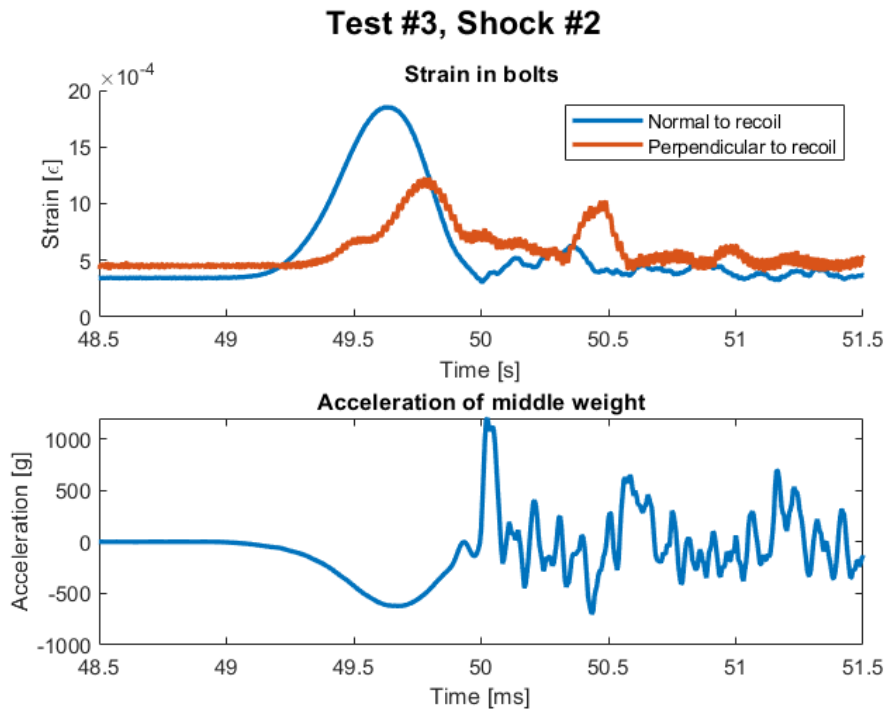


Figure 51: Strain measured in the bolts of each direction during the second shock of the third test and the accelerations from the middle weight of the fixture.

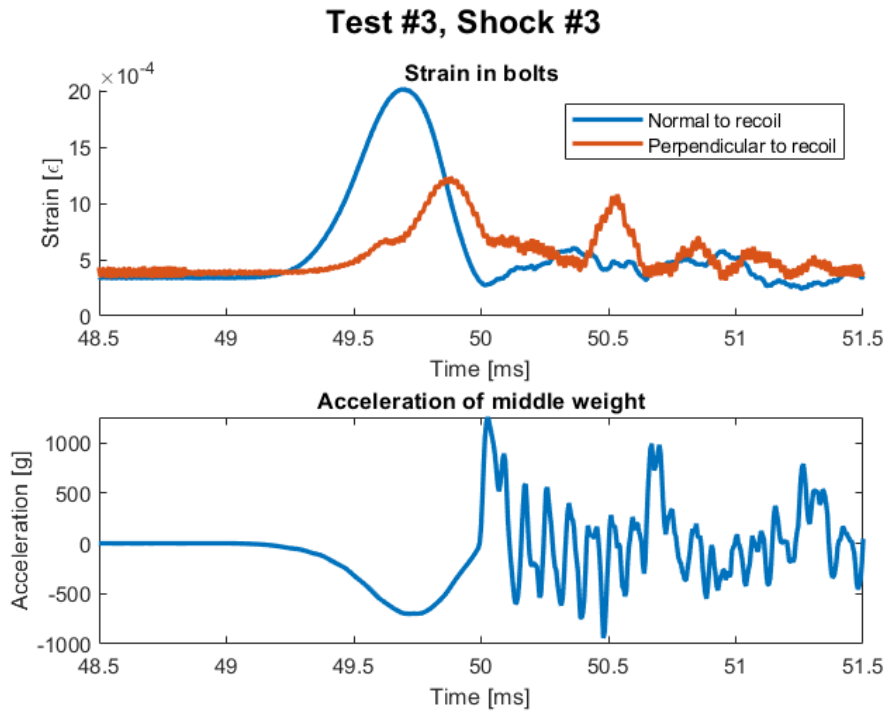


Figure 52: Strain measured in the bolts of each direction during the third shock of the third test and the accelerations from the middle weight of the fixture.